FACULTY OF INFORMATION TECHNOLOGY AND ELECTRICAL ENGINEERING
DEGREE PROGRAMME IN ELECTRONICS AND COMMUNICATIONS ENGINEERING

MASTER'S THESIS

IMPACT AND MODELING OF PHASE NOISE IN MILLIMETER WAVE BEAMFORMING SYSTEMS

Author	DEDAR RASHID
Supervisor	NUUTTI TERVO
Second examiner	KRISHNA CHAITANYA BULUSU
Technical advisor	BILAL KHAN

April 2023

Dedar Rashid. (2022) Impact and modeling of phase noise in mmW beamforming systems. Faculty of Information Technology and Electrical Engineering, Degree Programme in Electronics and Communications Engineering.

ABSTRACT

Due to the exponential growth of wireless communication, mobile communication applications require more bandwidth available in higher operating frequencies. High centre frequency makes the systems sensitive for phase variations caused by the phase noise (PN) of the imperfect local oscillators (LOs) used in wireless transceivers. Moreover, wide bandwidth also makes the faster phase variations of the phase noise spectra have an impact on the overall system performance by reducing effective signal-to-noise-ratio. These fast variations seen in the high offset frequencies in the phase noise spectra are typically ignored in the communication systems because the traditional system bandwidths are in order of megahertz, or in maximum few gigahertz. In mmW frequencies, i.e., at 30-300 GHz, the transceivers are typically using multiple antenna elements to achieve the required link range by highly directional beams. Often so-called phased arrays are used to implement the multi-antenna transceiver, where the beamforming is mostly performed in the analog domain by digitally controllable mmW phase shifters. For generating multiple beams from the same transceivers, more than one phased array is typically used in the same platform. The phased arrays often share a single LO, for multiple antenna elements. A typical LO generation architecture is containing a base clock, phased-locked loop (PLL), and some frequency multipliers to achieve the target mmW operating frequency. In multi-array systems, the LO signal can be divided into phased arrays in multiple domains, i.e., the arrays can have an independent clock, and a shared clock, but independent PLLs, shared PLL, or even the final mmW LO can be shared. In different architectures, the phase noise has different behavior, and it can have an impact for example on the beamforming accuracy. This thesis focuses on the effects of phase noise on milimeter-wave (mmW) beamforming systems to study different LO routing architectures. We mainly focus on LO architecture with multiple phased arrays that intend to make a common beamformer and their impact on overall system-level phase noise performance. The specific focus is given to the behavior of the wideband phase noise. The phase noise is modeled by using baseband equivalent models where a gaussian phase noise source is filtered by a filter modeling the equivalent phase noise spectra. The parameterization of the model is based on commercial LO phase noise spectra. The behavior is studied in different LO schemes in single-beam and multi-beam scenarios by using simple examples. The simulations are mostly carried out by using continuous-wave signals, but also the single-carrier modulated QAM waveform is demonstrated. The simulations are performed in MATLAB.

Keywords: Phase noise, local oscillators, arrays, frequency, antenna

CONTENTS

PREFACE

I am pleased to present my thesis which I wrote for my Master's degree in Wireless Communication Engineering at the University of Oulu, Finland. The completion of this thesis marks the end of a long and challenging journey which includes hard work, dedication, and enthusiasm. First of all, I am grateful to Allah almighty for giving me the strength to complete this thesis.

There are many people to whom I owe a great deal of gratitude for their support and guidance throughout the writing of this thesis. I am grateful to my supervisor, *Dr. Nuutti Tervo*, for his advice, expertise, and encouragement throughout this research process. His deep knowledge of the field and fruitful feedback were valuable in shaping my ideas and improving my work all the time. Also, I would like to acknowledge the support and mentorship of my technical advisor, *Msc. Bilal Khan*, during this research work as he worked above and beyond to assist and guide me in navigating the technical challenges I encountered during this time. I would also like to thank to my second examiner, *Dr. Krishna Chaitanya Bulusu*, for his valuable feedback and comments, which helped me to identify and address areas of improvement. I am also deeply grateful to the *Prof. Aarno Pärssinen*, for providing me with the opportunity and trust to pursue working on this project.

Moreover, I want to express my gratitude and acknowledgement for the unconditional love and support that my parents and family have shown me throughout my academic journey. In addition to their encouragement and sacrifice, I am forever indebted to their unwavering support.

Last but certainly not least, I express my sincere gratitude to the staff and colleagues at the Centre for Wireless Communications Engineering and my friends here in Oulu and back in Pakistan, who have been a constant source of supportive encouragement throughout this process. Having such amazing friends in my life has been an honour, and I am so thankful for their support.

Monday 3rd April, 2023, Oulu, Finland
DEDAR RASHID

LIST OF SYMBOLS AND ABBREVIATIONS

LO	local oscillator
PLL	phase locked loop
LPF	low pass filter
VCO	voltage-controlled oscillator
PFD	phase frequency detector
REF	reference
SSB	single side band
IF	intermediate frequency
RF	radio frequency
RMS	root-mean-square
LNA	low noise amplifier
PA	power amplifier
dB	decibel
dBc	In decibel scale, level relative to the level of carrier
dBm	In decibel scale, power relative to 1mW
OFDM	orthogonal frequency division multiplexing
SC	single carrier
QAM	quadrature amplitude modulation
EVM	error vector magnitude
CW	continuous wave
PSD	power spectral density
PN	phase noise
FOM	figure of merit
BS	base station
MIMO	multiple input multiple output
4G	fourth generation
5G NR	fifth generation new radio
PTRS	phase tracking reference signals
PRS	pilot repetition sequence
6G	sixth generation
mmW	millimeter-wave
SNR	signal-to-noise ratio
ABF	analog beamforming
ADC	analog-to-digital converter
DAC	digital-to-analog converter
MC	monte carlo
Hz	hertz
GHz	gigahertz
THz	terahertz

A_0	fixed amplitude
f_{osc}	oscillator center frequency
θ_0	fixed phase
A_{t}	random amplitude variation
θ_{t}	random phase variation
$L(f)$	power spectral density (PSD) of phase noise
P_{c}	carrier power

f_{c}	carrier frequency
f_{off}	offset frequency
N	total number of antenna elements in the array
$\overrightarrow{r_{\mathrm{n}}}$	relative position from origin of a given antenna element
$\overrightarrow{k}$	wave-vector of a plane wave in three orthogonal directions
k_{x}	x component of wave-vector
k_{y}	y component of wave-vector
k_{z}	z component of wave-vector
f_{z}	zero frequencies
π	ratio of a circle's circumference to its diameter
λ	wavelength
$\sum$	summation operator
d	antenna spacing
θ_{s}	steering angle
φ	azimuth angle
θ	elevation angle
‰	percentage
∞	infinity

1 INTRODUCTION

There has been an unprecedented rise in possibilities for the next generation of mobile networks as a result of millimeter-wave communication in recent years. The surge in data transfer speeds across both wired and wireless networks can be attributed to various technologies and devices, including tablets and smartphones, wireless and wired internet devices, machine learning, cloud, and machine-to-machine type communication, all of which have a substantial user base [1]. According to statistics, the demand for high data rates continues to rise, with an annual growth rate of approximately 60 percent.

Communication systems use oscillators to convert baseband signals into passband signals at the transmitter side and to convert passband signals back to the baseband at the receiver side [2]. Ideal oscillators produce sinusoidal waves with stable frequency and phase references. Nevertheless, practical oscillators combine passive and active elements. The thermal, shot and flicker noise in the circuit is caused by the movement of electrons and holes. A sinusoidal waveform produced by this oscillator is subjected to random fluctuations in phase caused by noise [3].

As wireless communication continues to grow exponentially, mobile communications applications required more and more channels in order to meet their needs. Due to these increased requirements, the phase noise (PN) of local oscillators has been subjected to a very high level of scrutiny [4]. Even though we live in a digital world, it limits the performance of the system, especially at higher frequencies where PN is more prevalent. The frequency of phase fluctuations [5] has been examined in a number of studies over the years. A significant reduction in the performance of a wireless communication system is caused by the phased noise that is generated by imperfect oscillators. The system performance becomes even more evident when operating at higher carrier frequencies, such as in the mmW range $30-100$ GHz and THz range over the 300 GHz [6]. An examination of the effect of PN on mmW systems is presented in this thesis.

As mentioned before, the communication systems are bound to experience PN as a result of the imperfections in the local oscillators, as the LO output signal is multiplied with radio frequency (RF) or intermediate frequency (IF) at the mixers to convert the baseband signal to the passband signal and vice versa [7]. As the name suggests, PN results from sudden deviation in the phase of a carrier wave, which can lead to significant increase in the power spectral density (PSD) of an output waveform. Ultimately, this can cause a significant decline in the system's overall performance on the grounds of partial loss of coherence between the channel estimation and the actual channel gain during the data transmission process [2]. This is even more evident when the system has to operate at higher frequencies, where the performance of the system becomes even more apparant. This thesis presents an examination of the effect of PN on mmW beamforming systems.

In order to provide a high capacity and data rate, mobile communication utilize millimeter-wave frequencies as a part of fifth-generation (5G) technologies. The development of advanced multibeam antenna systems as well as beamforming systems is essential to the advancement of 5G millimeter-wave mobile communications, as they enable higher gains, multiple streams of transmission, and a wider range of signal coverage. Despite this, with digital communication systems that operate at high data rates, PN is one of the most important factors to take into account. An oscillator at high carrier frequency will have a high PN level, such as E-band $60-100$ GHz, which has a more negative effect on high-carrier frequencies. Additionally, in orthogonal frequency division multiplexing (OFDM) systems, it is also possible to have an adverse effect on the orthogonality of subcarriers by causing interfaces between the subcarriers, which may negatively affect the performance of the system [8].

Millimeter-wave beamforming systems and how PN can be modeled and analyzed are important aspects of the development of high-performance communication systems. Considering

the higher-frequency range and the requirements for an accurate beamforming system are particularly challenging in terms of PN [9] - [10]. Developing new communication and sensing applications has been made possible thanks to the advancement in mmW technology. Beamforming systems have developed much popularity among researchers since mmW systems were introduced. Beamforming is a well-known method of improving the transmission efficiency of mmW technology and increasing the range of coverage offered by the technology. Despite of this, there is a strong correlation between the accuracy of the beamforming system and the PN system subjected to. As a result of phase noise, a beamforming system can perform less efficiently and have a negative impact on its quality [11].

This thesis thoroughly analyzes the effects of PN in mmW beamforming systems. The rest of the thesis is organized as follows. In Chapter 2 a detailed discussion of PN fundamentals, including its frequency and time domain behavior, as well as its modelling in Chapter 2. Furthermore, the generation of the LO signal heavily influences PN performance, and the LO signal generation using PLL has been discussed in Section 2.1. In Chapter 3 phased arrays are discussed as to how electronic beam steering is possible with antenna patterns. The section focuses on LO routing architectures for multi-array transceivers to assess the impact of PN on mmW phased array systems. The aim of this thesis is to analyze the impact of PN in LO routing architecture as well as their differences in the efficiency of PN based on the shared LO for multiple subarrays for arrays with a shared LO when the LO is shared between the multiple subarrays. A shared LO distribution network and an independent LO distribution network were discussed as LO strategies for multibeam systems. Several studies is carried out in order to demonstrate that PN can be a significant factor in the performance of multibeam combining systems. In a multibeam system, PN is spatially dependent on the LO distribution network, and different LO distribution networks affect the phase noise. Simulations are primarily conducted using continuous-wave signals. To showcase the impact for the real communication signal, single carrier (SC) quadrature amplitude modulation (QAM) signals are also analyzed in terms of error vector magnitude (EVM) as performance metric. All simulation has been performed in the MATLAB environment.

2 PHASE NOISE FUNDAMENTALS

This chapter covers the basic issues of PN in mmW communication systems. A variety of concepts are included under the heading of "frequency stability" including random noise, incidental modulation, and all other variations in an oscillator's output frequency. A source's frequency stability is determined by the consistency with which it produces sinusoidal frequencies over a given time period [12]. PN is a measure of the deviation of a periodic signal's phase from its ideal form. It is often expressed in terms of the root-mean-square (RMS) deviation of the phase over a certain time interval. PN is an important parameter in many systems, as it can limit the performance of such systems and introduce errors.
There are several factors that contribute to PN in a signal. The main source of PN is the noise present in the LO that generates the periodic signal. This noise can come from various sources, including thermal noise and flicker noise [13]. Other sources of PN include the noise introduced by the transmission and reception of the signal, as well as noise introduced by the components used in the system [14]. These sources of noise can be reduced by using high-quality components. There are several techniques that can be used to reduce PN in a system. One of the techniques is to use a phase-locked loop (PLL) to stabilize and generate a stable LO signal. A PLL consists of a feedback loop that compares the phase of a periodic signal to a reference signal and adjusts the phase of a periodic signal to match the reference.
In the design of any radio system, achieving the best possible performance from any radio system greatly depends on the generation of its LO signal [15]. It has become increasingly challenging for manufacturers to design phased array antenna systems that can take advantage of digital beamforming to process signal information in any way while taking advantage of the benefits of phased array antennas. As the number of transmitters and receivers increase, it becomes increasingly difficult to distribute LO signals and reference frequencies to a larger number of transmitters and receivers simultaneously. The system architecture will determine whether the LO frequencies will be distributed to a lower frequency reference, and the LO signal will be created at close proximity. Subsequently, it will be necessary to conduct an assessment of the PN that is generated at the system level by various distributed components and centralized components [13].

2.1 LO signal generation

Oscillators are autonomous electronic circuits that produce periodic, oscillating electric signals at precise frequencies. Communication systems use this frequency to transmit and receive passband signals, as well as provide timing and synchronization to the signals. There is a random amplitude and phase instability in the output signal of the oscillators used in communication transceivers [14]-[15]. The output of a reliable frequency source generates only one output signal with no instabilities in frequency or amplitude. All electronic circuits are susceptible to phase noise, interference and oscillators are no different. The first type of noise includes thermal noise and flicker noise, which are produced by various devices, while the second type includes supply noise and substrate noise. The oscillator output with phase noise can be written as [5].

$$[V_{\text{out}}(t)]_{\text{real}} = A(t)cos(2\pi f_{\text{osc}}t + \theta(t)), \tag{2.1}$$

where $A(t)$ represents the random amplitude variations. f_{osc} represents the center frequency of the oscillator, and $\theta(t)$ is random phase variation.
In communication systems, PLLs are commonly used for various purposes. One of the main uses is for frequency synthesis, where a PLL is used to generate a precise output frequency

from a lower-frequency reference input. PLLs are also used in radio communication systems as a local oscillator, whereas the LO output signal is multiplied with radio frequency (RF) or intermediate frequency (IF) at the mixers to convert the baseband signal to the passband signal at the transmitter side and passband signal into baseband signal at the receiver end [16]. Additionally, it can be used to synchronize, synthesize clocks, and reduced skew and jitter [17]. PLLs can also be used in modulation and demodulation schemes for digital communication systems to lock the phase of the transmitter and receiver. This circuit is formed by a feedback loop. Usually, in a PLL, the frequency and phase of the input signal are locked. It is widely accepted that PLLs can be used in advanced correspondence and instrumentation frameworks in several cutting-edge applications. Furthermore, PLLs are used to synthesize high clock frequencies from multiple low clock frequencies. PLLs are able to lock on signals with a bandwidth that fits within their ranges. At the input of PLL, the input or reference clock is compared with the feedback signal. It is continued until the phase and frequency of the signal have been locked [18].
There are several types of PLL circuits depending on the requirement for a given component. However, there are usually four components that are integrated into PLL circuit:

- Phase Frequency Detector (PFD).
- Low Pass Filter (LPF).
- Voltage Control Oscillator (VCO).
- Frequency Divider.

As shown in Fig.2.1. In the above Fig 2.1 the phase frequency detector (PFD) is the primary

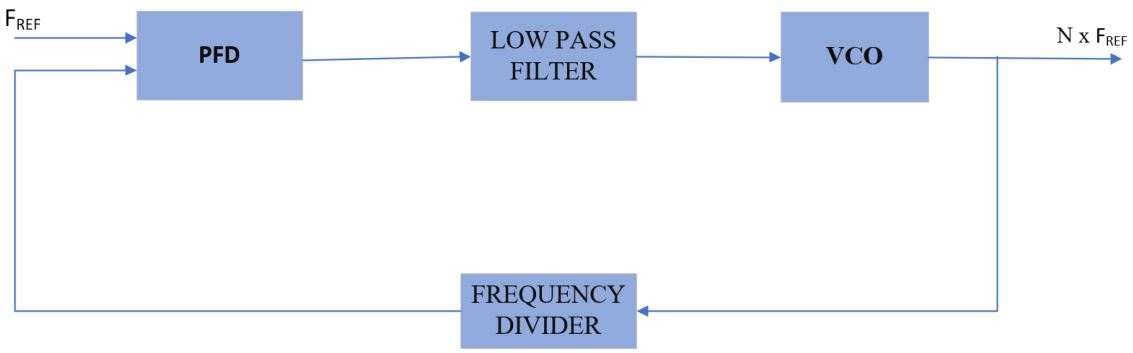

Figure 2.1: Basic PLL configuration. The output phase of a VCO is divided with a frequency divider, compared with an accurate reference signal, filtered, and fed back to theVCO control input.

crucial component of the circuit. The PFD evaluates the phase and frequency differences between the input F_{REF} and the feedback F_{REF}. These signals are compared by the PFD and produce two signal outputs, UP and DOWN, and these signal outputs are known as charge pumps (CP). By integrating the PLL low-pass filter into the charge pump output, the resultant charge pumps out high output current, increasing the tuning voltage of the VCO [13]. The VCO output voltage change depends on the output of PFD. In the case of PFDs, the UP generated at the output of PFD leads to an increase in phase and frequency values of the VCO as a result of an increase in the error voltage of PFD and vice versa.

In order to generate output frequencies that are multiples of the PFD frequency, PLL uses a feedback divider to divide the VCO frequency by the PFD frequency. It is also possible to use dividers in the reference path in order to use higher frequencies than those of PFD.

2.2 Frequency and time domain behavior of phase noise

2.2.1 Frequency domain

Phase noise is a form of random fluctuation in the phase of a periodic signal. In the frequency domain [19], PN appears as a distribution of spectral lines around the carrier frequency of the signal. These lines are usually referred to as sidebands, and their amplitude is a measure of the PN present in the signal as shown in Figure 2.2. It is typically expressed in dBc/Hz, which represents the amount of PN per unit frequency offset from the carrier frequency. The output of an ideal oscillator that oscillates with frequency ω_0 is an ideal periodic time function can be written as

$$[V_{\text{out}}(t)]_{\text{ideal}} = Acos(\omega_{\text{o}}t + \theta), \tag{2.2}$$

The Fourier expansion of such a function can be expressed as a series of Dirac Deltas at nω_0, since an ideal periodic waveform can be expressed as

$$[V_{\text{out}}(t)] = \frac{a_0}{2} + \sum_{1}^{\infty}(a_{\text{n}}.cos[n\omega_{\text{o}}(t)] + [(b_{\text{n}}.sin[n\omega_{\text{o}}(t)]), \tag{2.3}$$

The ideal oscillator has a constant amplitude and frequency, whereas the real oscillator's amplitude and frequency tend to vary around a certain average. the non-ideal waveform can be expressed as [20] follows

$$[V_{\text{out}}(t)]_{\text{real}} = A(t)cos(\omega_{\text{o}}t + \theta(t)), \tag{2.4}$$

Where A(t) and $\phi(t)$ are the time-varying amplitude and phase of the LO signal, respectively. Accordingly, the harmonics of an ideal oscillator are different from those of a real oscillator as shown in Figure 2.2. Both amplitude and frequency fluctuations cause the sidebands to appear as can be seen in Figure.2.2, these sidebands represent the PN sidebands to a great extent. Accordingly, PN can only be described by sidebands resulting from the frequency modulation of phase perturbations [21].

PN is typically quantified in terms of the power spectral density of the phase noise, denoted as $L(f)$ in units of dBc/Hz. The term dBc stands for decibels relative to the carrier, and Hz refers to the frequency offset from the carrier frequency. The PN power spectral density gives the amount of PN present at a given frequency offset from the carrier, so the PN in linear scale can be written as

$$L(f) = \frac{Noise\ Power\ in\ 1Hz\ Bandwidth}{Carrier\ Signal\ Power} \tag{2.5}$$

The PN in *dB* scale can be written as

$$L(f) = P_n(dBc/Hz) - P_c(dBm). \tag{2.6}$$

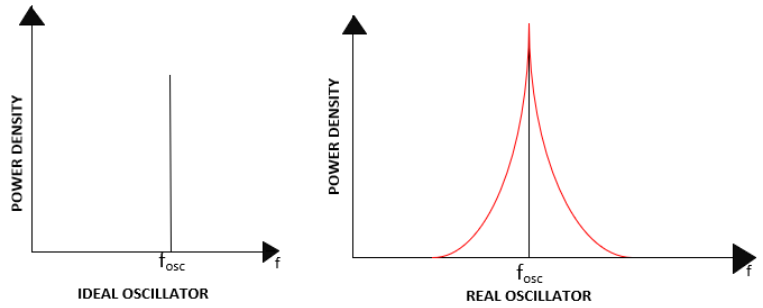

Figure 2.2: Frequency domain representation, of an oscillator that is free from noise (ideal) and operates at f_{osc}, as compared to a real oscillator.

In Equation 2.6, P_n is the phase noise in dBc/Hz, while P_c is the LO power in dBm. A single-sideband PN measurement is customarily used to characterize oscillators. The PN of an oscillator is mostly measured as a function of its frequency offset f_m as shown in Figure 2.3, where the frequency axis is plotted on a log scale [22]. There are several regions of the curve that have a slope of $\frac{1}{f^x}$, with $x = 0$ corresponding to the so-called "white" PN region where the slope equals to 0 $dB/decade$, and with $x = 1$ corresponding to the "flicker" PN region where the slope equals -20 $dB/decade$.

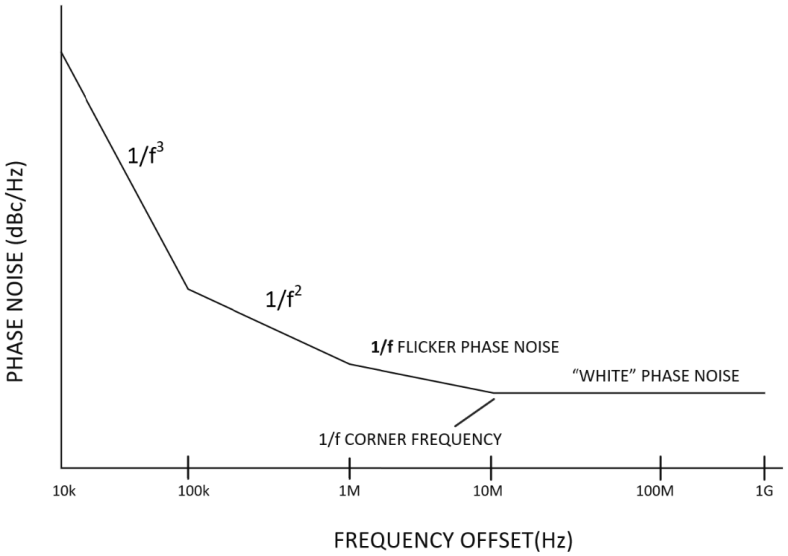

Figure 2.3: The oscillator phase noise curves, comprising white noise and flicker PN in dBc/Hz versus frequency offset in Hz, is depicted in this diagram.

2.2.2 Time domain

Phase noise can also be presented in time domain, when it is often called phase or time jitter [23]. In an ideal oscillator, the periodic time seems to be constant over time, while in a real oscillator, it fluctuates randomly. Typically, oscillators can be specified in terms of their PN

performance [17]. A typical graph is shown in Figure 2.4. It's important to note that the graph illustrates how the PN curve can be approximated with separate lines, and each of the endpoints is composed of a number of data points. In order to calculate equivalent RMS jitter, we first need to obtain the integrated PN power over the desired frequency range such that, the area under curve A. Each data point defines an individual area $(A1, A2, A3, A4)$ on the curve [22]. Fig 2.4, shows integrated PN power dBc and can be written as

$$A = 10\log_{10}(A1 + A2 + A3 + A4). \tag{2.7}$$

An individual power ratio can be obtained by integrating the power of each individual area. A power ratio that is determined by each individual power ratio is then added up and converted back into *dBc* values. A phase jitter in radians can be calculated from the integrated PN power as

$$\alpha_{rms}(rad) = \sqrt{2 \times 10^{\frac{A}{10}}}. \tag{2.8}$$

by dividing Equation 2.8 with $2\pi f_0$, the phase jitter (radians) can be converted to time jitter (seconds) as

$$\alpha_{rms}(sec) = \frac{\sqrt{2 \times 10^{\frac{A}{10}}}}{2\pi f_o}. \tag{2.9}$$

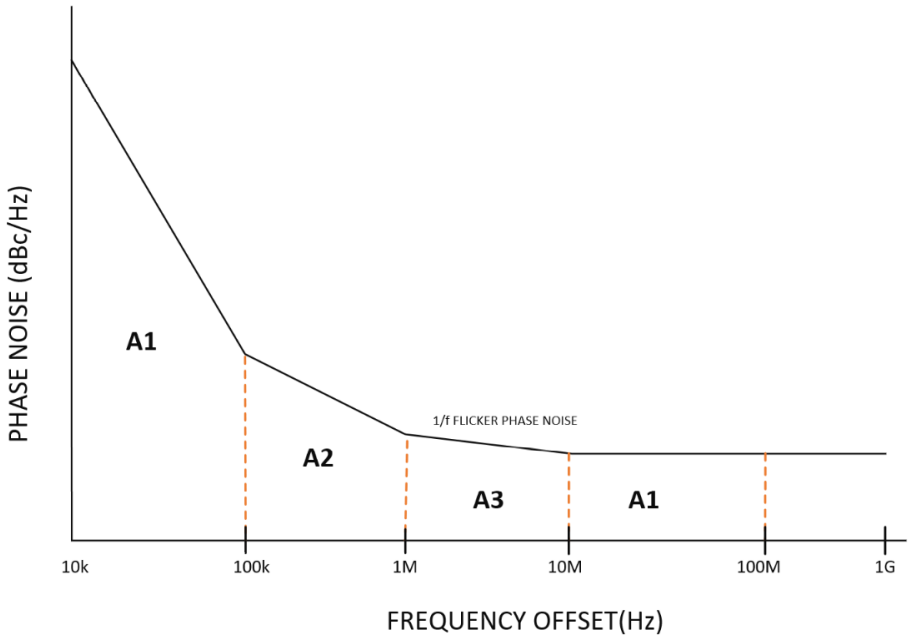

Figure 2.4: This Figure illustrates calculating jitter from phase noise

2.3 Phase noise model

In this thesis, we used the 3rd generation partnership project (3GPP) phase noise model [24]. The PN model is a mathematical representation of the variations in the phase of a signal as it travels through a system or component. The model takes into account factors such as noise sources, frequency, and time. The response of the PN model depends on the specific parameters used in the model [12], as well as the specific system or component being analyzed. Some common responses include the PN power spectral density, the phase jitter, and the phase error. These responses can be used to understand how the system or component may perform under different conditions and can aid in the design and optimization of the system or component [5]. In this thesis, we have considered a local oscillator based on PLL that is widely used in transceivers. As discussed earlier in Section 2.1, PLL-based LOs are subjected to three main sources of phase noise, namely, noise caused by reference oscillator, PFD, loop filter, and noise from VCO as shown in Figure 2.1. The model for the equivalent filter of the phase noise spectra in frequency domain is expressed as

$$S_{\text{Total}}(f) = \begin{cases} S_{\text{ref}}(f) + SPLL(f), \text{ when} f \leq LoopBW \\ S_{\text{VCO\_v2}}(f) + SVCO\_v3(f), \text{ when f} > \text{Loop B} \end{cases} \tag{2.10}$$

where

$$S_{\text{Ref/PLL/VCO\_v2/VCO\_v2}} = PSD0. \left[\frac{1 + (\frac{f/f_z}{f})^k}{1 + (f^k)} \right] (dB). \tag{2.11}$$

and

$$PSD0 = FOM_{\text{VCO\_V2}} + 20 \log f_c - 10 \log(\frac{P}{1mW})(dB). \tag{2.12}$$

Parameters shown in the table above 2.1 are used to evaluate the performance of the system. The

Table 2.1: Parameters of the 3GPP phase noise model [24] used in the simulations

Model 2 BS LoopBW= 112k				
	REF Clk	PLL	VCO V2	VCO V3
FOM	-240	-240	-187	-130
f_z	infinite	1.00E+04	8.00E+06	infinite
P (mW)	10	20	50	50
k	2	1	2	3

figure of merit (FOM) can be determined by considering various factors such as cost, accuracy and power consumption, f_c represents carrier frequency and P is consumed power. The proposed PN model at the base station (BS) side has been designed to meet specific parameters, such

as PN level, carrier frequency, and power consumption as shown in Table 2.1. PN is typically measured in decibels relative to the carrier frequency and is often expressed in terms of PSD. The PSD of the PN is usually plotted on a logarithmic scale, with frequency offset from the carrier on the x-axis and the PN level on the y-axis. The Figure 2.5 shows the PSD of this PN model at carrier frequency 300 GHz. Figure 2.6, shows the equivalent filter for phase noise

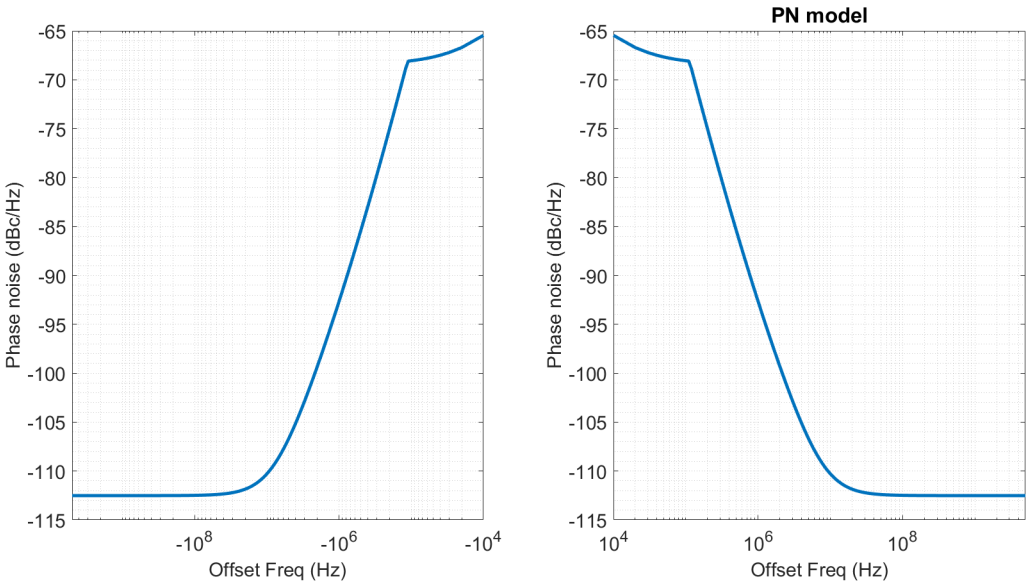

Figure 2.5: This Figure shows the PSD of phase noise model at 300 Ghz.

[25], that makes the desired PN spectra from the gaussian phase noise source. In Figure 2.6, the mathematical expression $\phi_w(n) \sim \mathcal{N}(0,1)$, states the phase of the white noise signal, follows a normal distribution with a mean of 0 and variance of 1, while $H(f) = \frac{1}{\sqrt{2}}\sqrt{S(f)}$, represents a transfer function at frequency f and $S(f)$ is the PSD of the phase noise at frequency f. The $\phi_{LO}(n)$ represents the phase noise signal. The phase noise spectra can be filtered by generating

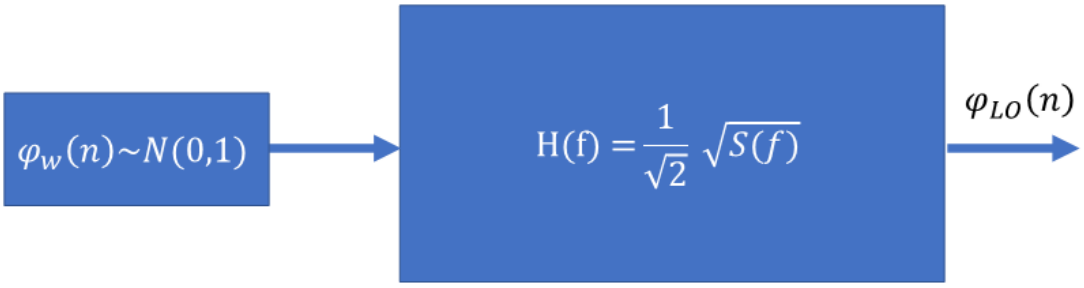

Figure 2.6: The Figure illustrates the equivalent filter for phase noise, that makes the desired PN spectra from the gaussian phase noise source.

normally distributed phase noise. Fourier transform can be used to represent this which can be written [25] as

$$\phi_{LO}(t) = \int_{f_1}^{f_2} H(f)\phi_w(f)\exp(2\pi ft)df \tag{2.13}$$

where $\phi_w(f)$, is the white gaussian noise signal over a frequency range from f_1 to f_2, f_1 is the smallest frequency that matters and f_2 is the higher frequency where the PN model applies, and applying an exponential factor $\exp(2\pi ft)$, to account for the time-varying nature of the carrier signal.

3 MILLIMETER WAVE PHASED ARRAY SYSTEM AND LO ROUTING ARCHITECTURES FOR MULTI-ARRAY TRANSCEIVERS

Wireless communication systems have become increasingly dependent on modern mmW phased array systems, which are becoming more and more crucial in the world of imaging and communication systems [26],[27]. The next section discusses phased arrays and how electronic beam steering can be accomplished with antenna patterns. This chapter also focuses on the study of LO routing architectures for multi-array transceivers to assess the impact of PN on mmW phased array systems.

3.1 Phased Arrays

As mentioned earlier, an antenna array is a collection of antennas arranged geometrically. An antenna array can be classified into two types: those with fixed main beam direction and those with steerable main beams by varying phases between antennas, this is referred to as phased arrays [26]. It is important to note that antenna arrays have the advantage of being able to produce highly directive beams, and as a result, they can increase a communication system's link budget. In modern communication systems such as 5G, utilizing antenna arrays is of key importance in order to overcome the high propagation losses that occur at high frequencies. In order to ensure that the beam of the mobile platform and a base station are aligned when the user is moving, beam steering is necessary [27]. Several techniques are possible with antenna arrays, including multiple-input multiple-output (MIMO), which allows for simultaneous transmission and reception of information via multiple antennas, and spatial filtering, which reduces interference caused by ambient noise. Electronic beam steering [28] can be accomplished by either varying the phase of the RF signals in each path of the antenna element or by altering the relative delay between the signals in each path of the antenna element. Analog or digital tuning can be used to adjust the delay or phase [29]. Typically, each antenna element is equipped with a phase shifter in mmW frequencies. Analog beamforming is emphasized in this thesis, which is a method used in mmW communication systems to direct beams towards a specific direction. This is typically achieved by using an array of antenna elements, each of which can be individually controlled to vary the phase and amplitude of the signals being transmitted or received by the antenna [29],[28]. Analog beamforming is typically used in mmW systems because it allows for the use of numerous antenna elements, which is necessary to achieve the high gain and directivity required for communication at mmW frequencies [30]. Array factor can be calculated by deriving the following formula

$$AF(\phi,\theta) = \sum_{n=1}^{N} e^{-j\,\overrightarrow{k}\,(\phi,\theta).\overrightarrow{r_{\mathrm{n}}}}. \tag{3.1}$$

In equation 3.1, N represents the total number of antenna elements in the array [30], while $\overrightarrow{r_{\mathrm{n}}}$ represents the relative position from the origin of a given antenna element. In general, the term $\overrightarrow{k}$ can be described in three orthogonal directions (along x, y and z axis) [31] as shown in the equation 3.2 can be written as

$$\overrightarrow{k}\,(\phi,\theta) = (k_{\mathrm{x}}, k_{\mathrm{y}}, k_{\mathrm{z}}) = \frac{2\pi}{\lambda}(\sin\theta\cos\phi, \sin\theta\sin\phi, \cos\theta). \tag{3.2}$$

where ϕ and θ are the azimuth and elevation angle, respectively. In order to steer the beam to a required direction [32] can be calculated as

$$\Delta\phi_{\mathrm{PS}} = \frac{2\pi}{\lambda} d.\sin(\theta_{\mathrm{s}}). \tag{3.3}$$

In equation 3.3, d is the antenna spacing, λ is the wavelength and θ_s is the desired steering angle. This means that the next phase shifter will adjust the phase delay between the output signals from each of the element. It will ensure that are all in phase with one another so the output signal travels in the same direction as one another. With a large array gain, it is possible to obtain a coherent output signal by summarizing the signal of each element [30]. The other incoming signals, which will come in from a different angle, on the other hand, will not be summarized coherently at the array output. This will result in significant attenuation in the output signal. Every communication system is composed of several components, each of which plays an important role in the data stream transmission from one point to another point. An illustration of a typical phased array transmitter and receiver is shown in Figure 3.1.

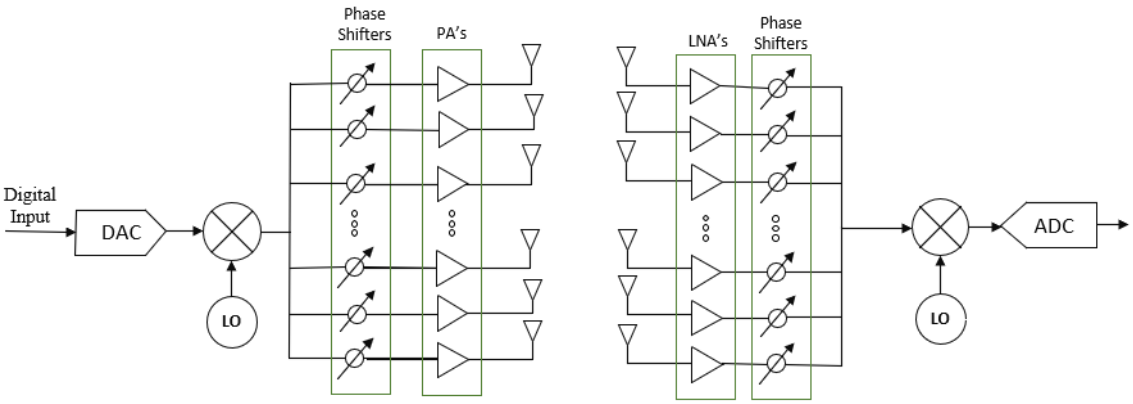

Figure 3.1: An illustration of a typical phased array transmitter and receiver.

3.2 Different LO Strategies for Multi-Beam Systems

There are several ways to implement LO generation and distribution. Different LO strategies have advantages and disadvantages in performance, area, power consumption, complexity and cost. There are two types of oscillators that are most commonly used, free-running oscillators and phased-locked loop oscillators. Phase locking is a method in which a system suffers from a very low PN, which can be understood as a zero mean stationary random process. The PN resulting from a free-running system is modelled as a Wiener process that contains a Gaussian distribution [33],[34] of increments between sampling instants.

According to the transceiver architecture and implementation, the PN between different RF chains can be correlated when all its RF chains are capable of sharing the same LO. Therefore, all of its RF chains also experience the same rotation at the same time. Conversely, when each RF chain is equipped with its own LOs and is equipped with independent RF chains, the PN is uncorrelated [35].

A number of different distribution architectures for LOs are presented in Figure 3.2 [6]. A

common LO is distributed to each antenna element can be seen in Figure 3.2a, with the desired PN profile. Therefore, a large amount of power will be consumed by the LO distribution buffers in this scenario in order for the network to overcome the large losses associated with LO distribution to each element. Another approach is to use separate LO for each antenna element as shown in Figure 3.2b. Due to the short mmW distribution, the power consumption in this scenario is dominated by LOs. However, by averaging the uncorrelated noise of individual oscillators, one will be able to determine that the combined power of the VCOs in independents equals the combined power of all the VCOs in commons [36].
There are several disadvantages of this solution, including the mismatch between the VCOs. An alternative but the more robust method is generating a superior quality LO signal through PLL and distributing it to mixers to produce a reliable LO signal, as shown in blocked-based LO in Figure 3.2c.

3.3 Shared LO and Independent LO Distribution Network

In this thesis, we are considering two types of LO routing, shared and independent, as discussed in the previous section. Considering a shared LO case, we assume that we have a common LO signal having the same path length serving two phased arrays in the far field, and in the later case, we will also see the independent LO distribution. Fig 3.3, represents the transmission side block diagram for two paths that shared a typical LO. We have generated the LO signal using PLL which acts as a feedback control system as shown in Fig 2.1. The architecture consists of a charge pump, and PFD has been used in PLLs; PFD is used to detect frequencies when out-of-phase and acts as a phase detector when the loop is locked. The charge pump (CP) converts the PFD's digital pulses into current pulses, which are then injected into the loop filter. CP pulses are then attenuated by the loop filter, resulting in a control signal to the VCO. The VCO generates an RF output signal. This signal is then divided by a frequency divider and compared to the reference signal in the PFD, closing the feedback loop. The LO signal is then distributed in different paths and then uses a multiplier to generate a high-frequency/desired LO signal. Considering that normally the PLL operates at a lower frequency rather than desired LO frequency. The carrier-generated LO signal is then multiplied with the IF or baseband signal at the mixer to generate the RF signal. The RF signal is then fed into the phased array model which is given as $H(f, \varphi, \theta)$, where we assume that the channel is narrowband and φ, θ represents the azimuth and elevation angle at the receiver end. The resultant signal from different paths is added at the summing node before sending it to the far field where the phased array serves a user. The IF signal is given in equation 3.5.
The same scenario for the transmission side can be seen in Figure 3.4 where an independent LO signal is shared to each mixer rather than common as shown in Figure 3.3. Let us denote the LO signal with PN which can be written as

$$x_{\mathrm{LO}}(t) = exp^{(j2\pi fc+\phi_i)}. \tag{3.4}$$

Where f_c is the carrier frequency, ϕ_{i} is the phase shift at carrier frequency. The IF signal can be written as

$$x = exp^{j2\pi f_{\mathrm{o}}t}. \tag{3.5}$$

In Equation 3.5, f_o represents baseband frequency and t represents the time. Note that here we assume that input signal is continuous wave signal, in a later case we also simulate our simulator

with modulated QAM signal to see the behavior of phase noise.

The independent LO case can be seen in Figure 3.4, where a separate LO/PLL is used for each phased array. In order to produce the desired LO signal, a multiplier is used in each path to achieve the desired LO signal, followed by a mixer where the carrier LO signal is multiplied by the IF signal to generate the RF signal. After each path has generated its resultant signal, the resultant signals are then combined in the user direction in the far field where it served a user.

At the receiver end, Figure 3.5 shows a receiver with two phased arrays; each array is equipped with an antenna and low noise amplifier (LNA) and phase shifter where the analog beamforming is performed for each phased array. The two phased arrays are then connected to separate mixers where a shared LO signal is multiplied by the RF signal to get the IF or baseband signal. The output signal from the mixers is then passed through an LPF to remove unwanted high-frequency components that might have been introduced during the processing, and it helps to make sure that only a required one has to pass through an analog-to-digital converter. The ADC is then used to convert the analog IF signal to a digital signal use techniques such as digital beamforming can be used to process digital signals to extract the desired signal from the noise and interference in the signal.

The same scenario can be seen in Figure 3.6, but having independent LO/PLLs rather than common LO is being shared with each mixer. In later simulations, we will see how we can use both shared and independent LO cases or methods to reduce PN as it limits signal quality, especially in higher carrier frequencies and having wider bandwidths. We will also see if we can improve SNR with more than two paths. Also, we will also perform the simulation with modulated signal and will analyze how the PN can affect/ reduce the error vector magnitude (EVM) at the receiver end.

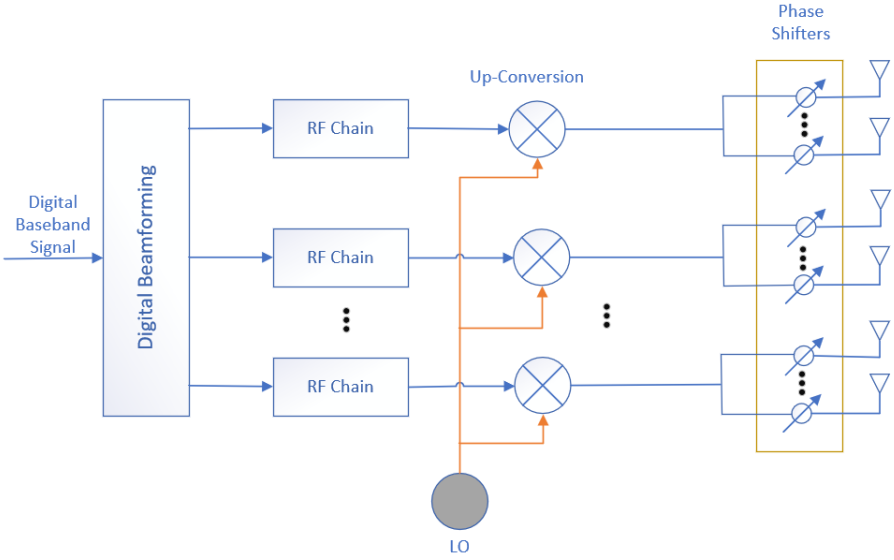

(a) Common LO

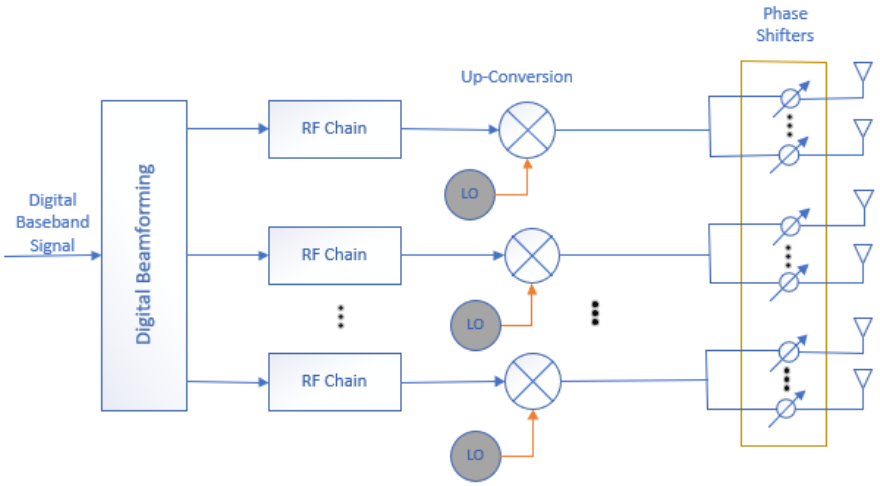

(b) Independent LO

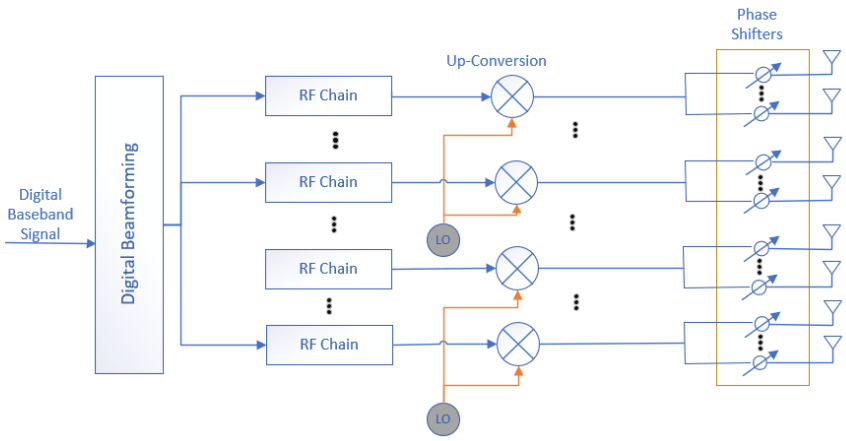

(c) Blocked-based LO

Figure 3.2: Three alternative LO routing strategies for multi-array system [6]: (a) common LO, (b) independent LO, and (c) block-based LO scheme.

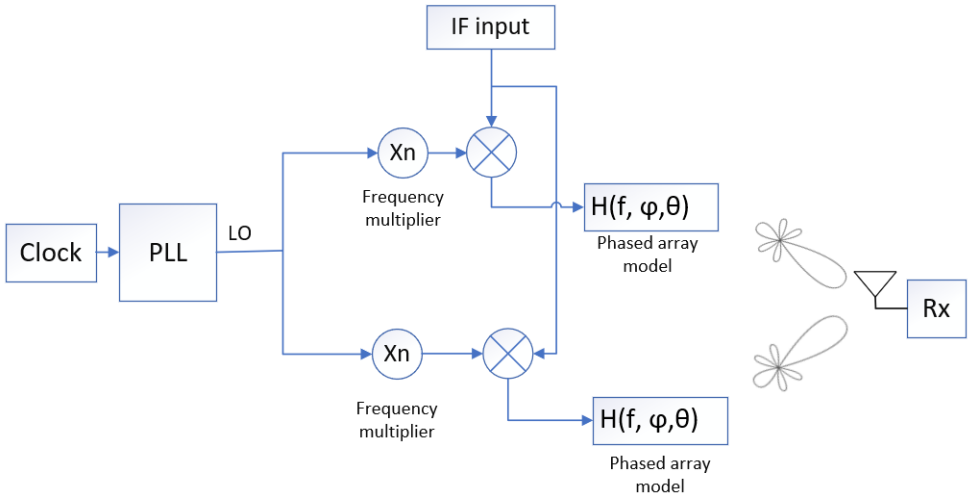

Figure 3.3: Shows transmission side block diagram of the model, two paths share a common LO and then multiplied with a multiplier in order to get the desired LO signal, followed by a mixer where the carrier LO signal is multiplied with the IF signal to generate the RF signal. After each path has generated its resultant signal, the resultant signals are then combined in the user direction in the far field where it served a user.

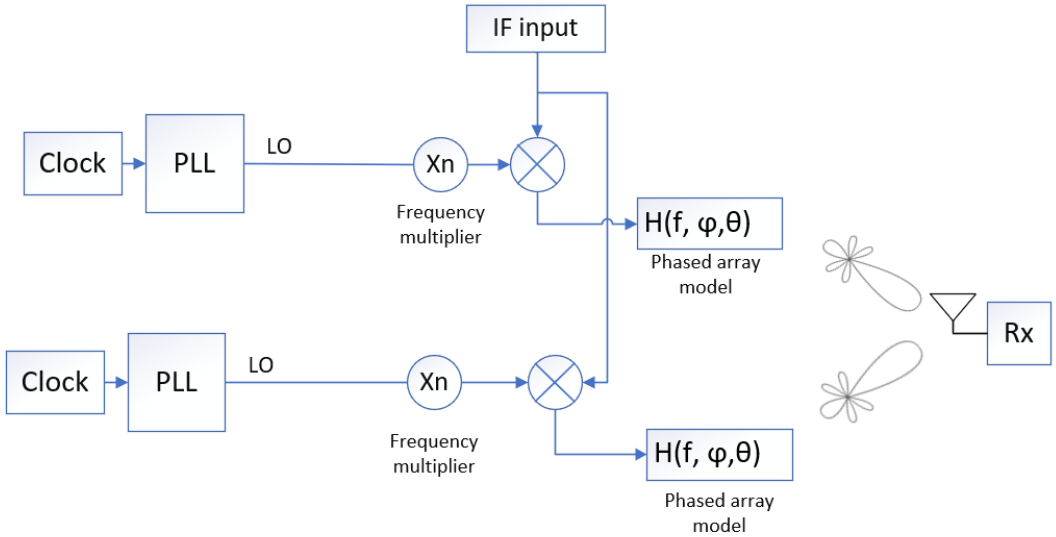

Figure 3.4: Shows transmission side block diagram of the model, two paths having an Independent LO signal with the same path lengths and then the LO signal is multiplied with a multiplier in order to get the desired LO signal, followed by a mixer where the LO signal is multiplied with the baseband or IF signal. After each path has generated its resultant signal, the resultant signals are then combined in the user direction in the far field where it served a user.

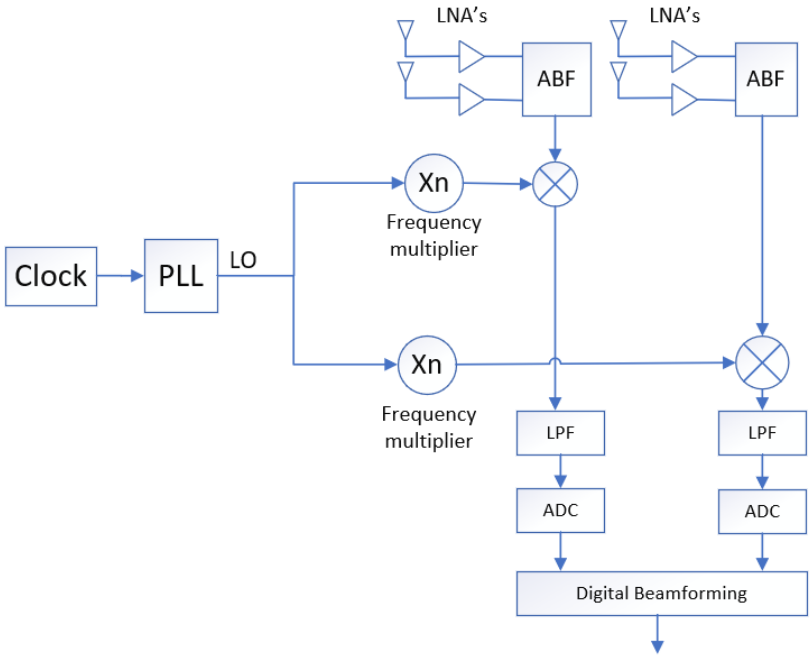

Figure 3.5: Shows receiver side block diagram of the model, two paths shared a common LO signal which is then with same path lengths to two separate mixers and multiplier is being used in each path to get the desired LO signal. The IF signal is then generated by mixing the LO signal with the incoming RF signal and then passing through LPF which helps to make sure that only the desired signal is passed to ADC which converts the IF signal to a digital signal.

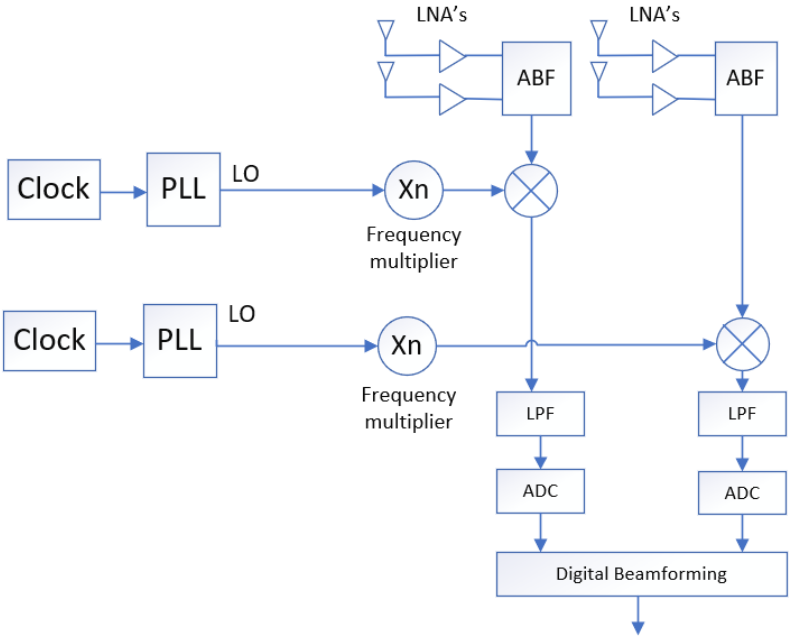

Figure 3.6: Shows receiver side block diagram of the model, two paths shared an independent LO signal which is then with same path lengths to two separate mixers and multiplier is being used in each path to get the desired LO signal. The IF signal is then generated by mixing the LO signal with the incoming RF signal and then passing through LPF which helps to make sure that only the desired signal is passed to ADC which converts the IF signal to a digital signal.

4 PHASE NOISE ANALYSIS IN MULTI-BEAM SYSTEMS

There has been an unprecedented rise in possibilities for next-generation mobile networks as a result of millimeter-wave communications in recent years. In the mmW system, frequencies range from 30 GHz – 300 GHz. The next-generation wireless communication system will provide high gigabits per second (Gbs) at mmW frequencies. When compared to the 4G system, millimeter waves have a higher frequency range [9]. Many users require a faster and more spectrum-efficient communication system to handle applications with higher data rates. The actual performance of real communication systems can vary depending on the assumptions that are made about the imperfections in the system design, such as channel estimation errors and hardware limitations, but these can still outperform the capacity limits [37]. A major problem that modern digital communication systems face is the existence of oscillator phase noise, which is becoming a limiting factor when it comes to high data rate systems that employ dense constellations that are severely hampered by phase noise, limiting the performance significantly [12].
Phase noise increases with an increase in carrier frequency, so systems with high carrier frequencies may suffer from worse phase noise. In mmW, using higher frequencies results in significant phase noise, shadowing, attenuation, and path loss. A major disadvantage of mmW is a significant increase in PN that occurs due to high carrier frequencies, which adversely affects the system performance [38]. A communication link's performance is significantly affected by PN. The multiplicative nature of PN makes it difficult to counteract additive noise by increasing the power of the signal [39]. The result of this is that it leads to distortions that scale with the power of the signal, and subsequently, the performance floor of an oscillator can only decrease by reducing the power of the oscillator in order to reduce distortion.
In the multibeam PN can have a significant effect on the performance of a communication system, and therefore it is crucial to analyze and understand the optimal performance. It can be due to multiple factors, such as thermal noise in the LO signal. In the Sections 4.2 - 4.3, different LO architectures were studied for both shared LO and independent LO cases. Also, the simulations are performed with continuous wave signals and as well as with single-carrier QAM waveform.

4.1 Spatial Behavior of Phase Noise

As discussed earlier, the PN of a signal can be defined as the random fluctuations of a signal phase over time. This random fluctuation can negatively impact the performance of a multibeam system depending on the way the beams are aligned as it cause error in steering direction, resulting in reduced gain and increased interference in the communication system [40]. PN can be measured at different points within the system or can be predicated by simulations and mathematical models. The level of PN can visualize by its PSD. LO sharing strategy has major impact on the spatial behavior of the phase noise. This is due to the fact that it determines whether the phase noise is similar over the antenna paths or not. The LO sharing strategy is highly dependent on the overall beamforming architecture, i.e. weather the antenna paths have the same or different digital signal chain. In the literature, these are often referred to as fully digital beamforming [41], analog beamforming, or a mixture of them, often called as hybrid beamforming [42]. In this thesis, we mainly focus on architecture with multiple phased arrays that intend to make a common beamformer. In the next sections, a detailed discussion is covered for both shared and Independent LO case that how we applied phase noise compensation approach. In later sections 4.2 - 4.3, a detailed discussion is covered for both shared and Independent routing along with the comparison of simulation results, and we also discussed how it affects the PN. Furthermore,

we also compared both shared and independent LO cases with two different signals, such that in case one we assume we have the baseband input to be a continuous wave signal, and secondly we assumed that we baseband signal is a modulated QAM signal to see PN behavior.

4.1.1 Phase noise compensation technique

Phase noise is critical in a multibeam system because it affects the phase stability of beams and, as a result, impacts the quality of the combined beam at the receiver end. To tackle this problem, the receiver can be more robust in estimating the carrier phase by introducing array level PN compensation technique which use lower offset frequency pilot symbols into the data sequence [43]. The pilot repetition sequence (PRS) periodically transmits a repetitive set of predefined values. The PRS allows the receiver to estimate the PN introduced during transmission. Reference signals are generally used in frame structures of various waveform types. For example, PTRS is used in 5GNR systems for phase tracking [44],[45]. The receiver can use periodic transmissions of the known values to determine the phase error introduced by comparing the received values with the expected values. As a result, the received signal can be adjusted, and PN can be compensated for by using this phase error. In this section, we have considered two scenarios for PN compensation using PRS and see how we can get some benefit at the user end. Firstly, the first received signals from the phased arrays are summed and then compensated for the PN for lower offset frequencies. Secondly, we compensate for received signals separately and then combine the resultant signal as for the shared LO case it can be seen in Figure 4.1, and for the independent LO case it can be seen in Figure 4.2. The same scenario is also repeated for the four phased arrays also and results are discussed later in this chapter.
Figure 4.3, shows phase noise cancellation is performed in the time domain and the running

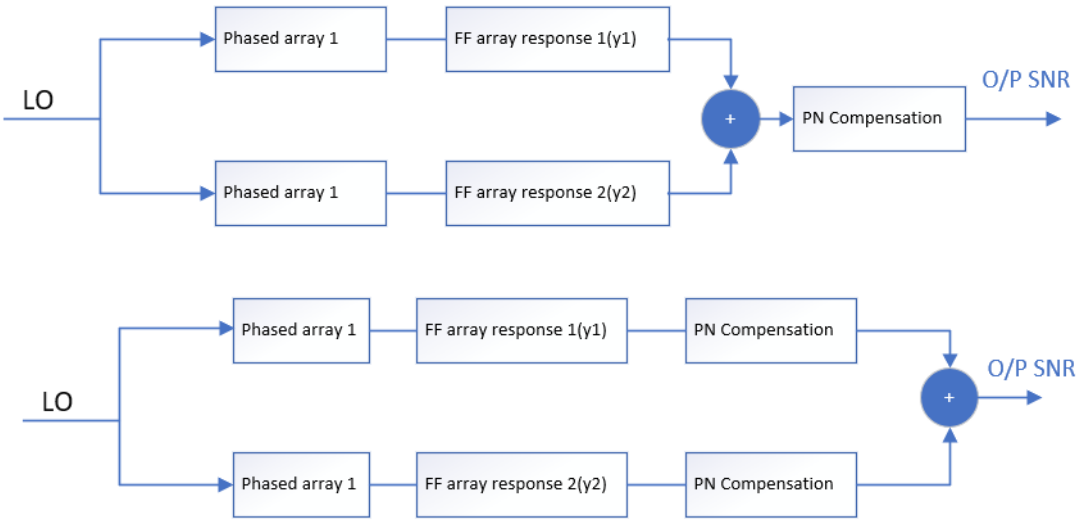

Figure 4.1: This figure shows PN compensation approaches applied for shared LO case. Firstly, the first received signals (y1 and y2) from the phased arrays are summed and then compensated for the PN for lower offset frequencies. Secondly, we compensate for received signals (y1 and y2) separately and then combine the resultant signal at the receiver end.

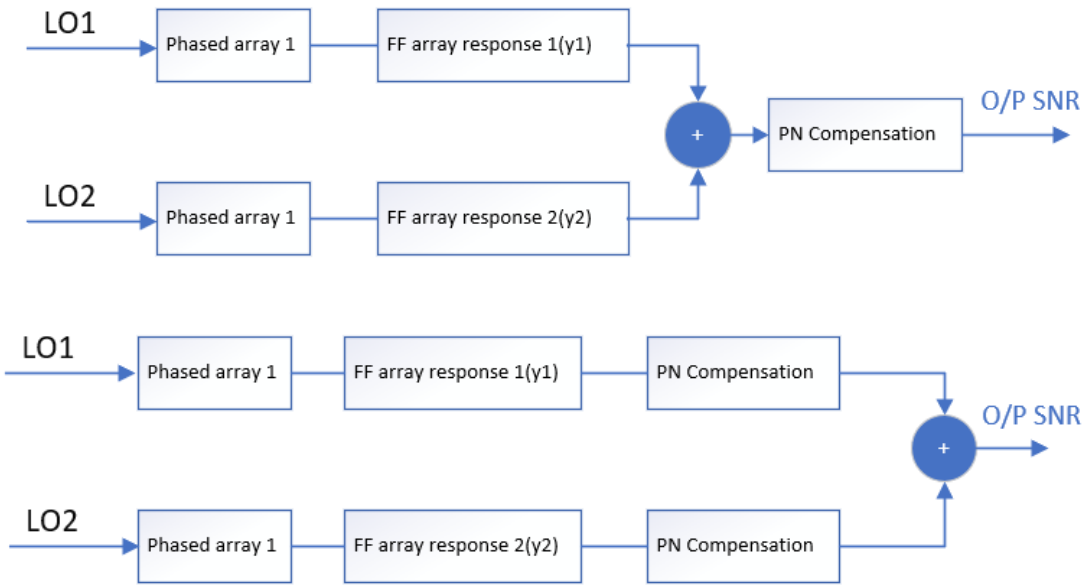

Figure 4.2: This figure shows PN compensation approaches applied for independent LO case. Firstly, the first received signals (y1 and y2) from the phased arrays are summed and then compensated for the PN for lower offset frequencies. Secondly, we compensate for received signals (y1 and y2) separately and then combine the resultant signal at the receiver end.

mean average is used over 10 samples having a cutoff frequency of 8 Mhz. The average running mean helps smooth out noisy data [46]. Using the average mean over ten sample means, which make a fixed-size window, we calculated the mean of the first 10 data points, then the mean of the second through eleventh data points, and so on. The window size remains constant at 10, and the mean is calculated for each consecutive set of 10 data points.

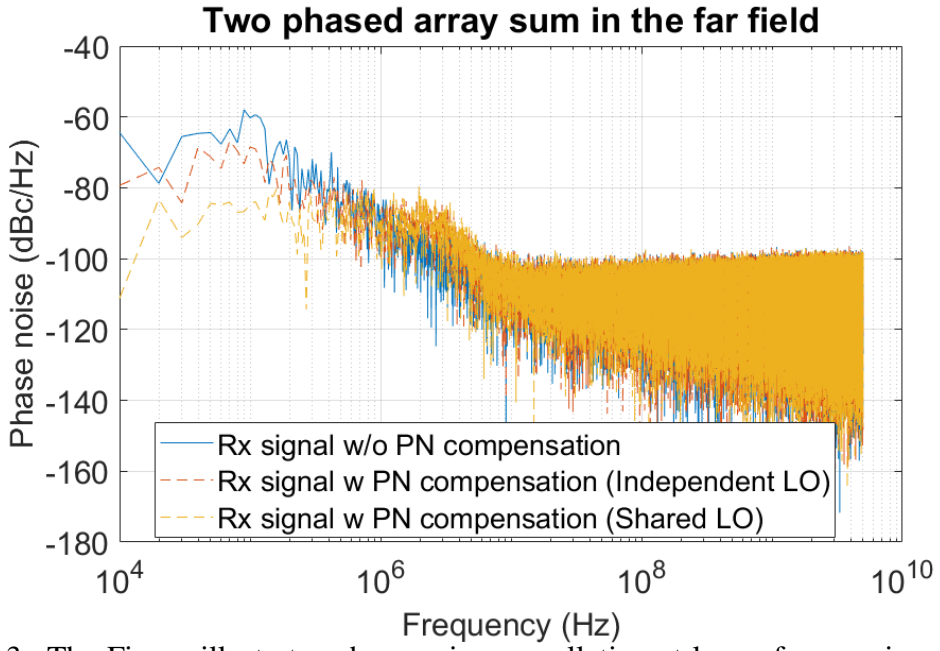

Figure 4.3: The Figure illustrates phase noise cancellation at lower frequencies and response without and with PN cancellation for both independent and shared LO cases in time domain.

4.2 Phase Noise in Multi-Beam Combining with Shared LO Distribution

In Section 4.2.1 we run the simulations to model the effects of PN in multibeam combining with shared LO distribution. In this simulation, we have used the PN model which is demonstrated in detail in Section 2.3 and the model can be seen in Figure 2.5 with having simulation parameters bandwidth of $F_s = 10\,\text{GHz}$ carrier frequency $F_c = 300\,\text{GHz}$. In Section 4.2.2, the simulations have been carried out with more complex signals such as 16-QAM signal with root raised cosine (RRC) pulse shaping having roll-off factor of (0.35) and symbol rate of 1 GHz. The oversampling factor with pulse shaping filter is four which results in four samples per symbol. Furthermore, received signal constellations and the corresponding EVMs are also calculated.

4.2.1 Simulations with continuous wave

Figure 4.4, shows the received LO phase noise spectra of two phased arrays sum in the far field for shared LO case when there is no phase noise compensation involved. As can be seen from the spectrum in Figure 4.4, the actual signal in the main band i.e, at 300 GHz and the noise on the rest of the band from low frequency (295 GHz) to high frequency (305 GHz) and the SNR is calculated over the entire 10 GHz band. As can be seen in Figure 4.4 having the SNR value roughly of 12 dB. As the SNR is dominated by the PN at low offset frequencies, PN cancellation is needed for these lower offset frequencies to see the actual SNR improvement.

As discussed earlier in Section 4.1.1, here the focus is on two different scenarios; Firstly, the

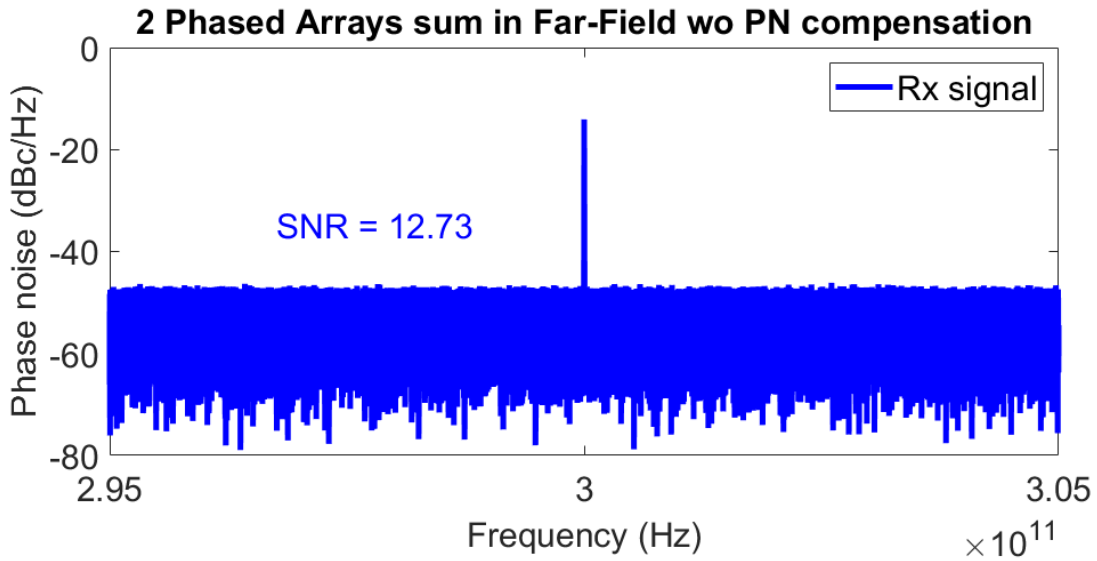

Figure 4.4: Received LO phase noise spectra of two phased arrays sum in the far field for shared LO case when there is no phase noise compensation.

array responses are added, and then the phase noise compensation technique is applied to the resultant signal for both two phased arrays and four phased arrays for shared LO cases where the same LO signal is shared for both two and four phased array cases. Figures 4.5 - 4.6, shows the received signal spectrum for two phased arrays and four phased arrays with shared LO where array responses are first added at the receiver end and then the resultant signal is

being compensated for lower offset frequencies respectively. Secondly, the PN compensation is applied to each array independently and then summed together to get the resultant received signal at the receiver end as shown in Figure 4.7 which indicates the case for two phased arrays and Figure 4.8 for four phased arrays scenario. Applying the array-level compensation technique as explained in section 4.1.1 , we have seen around 3 dB SNR improvement with respect to the case when we don't have any array-level PN compensation for lower offset frequencies. Furthermore, we do not get any benefit from the shared LO case where we applied independent compensation for both two array cases and four arrays cases, as it can be seen that there is no change in SNR values and also on the noise floor level concerning the case where PN compensation is applied after adding the array responses due to the fact the noise source is correlated, by adding the signal also add the same noise and the ratio remains the same and that's why we don't get any benefit. However, the power level of the signal in the main band, i.e., at 300 GHz, is different in different cases for two-phased array cases; the power level is -34 dB, and for four-phased array cases the power level is -28 dB is due to the fact that the noise power in the resulting signal will increase linearly with the number of signals combined, if the combined signals are of the same amplitude and fully correlated with each other, i.e., their noises are also perfectly correlated. In this simulation where signals are added, for example, the noise power in the resulting signal will be twice of each signal individually if they are added together. This is because the noise power of each signal will be increased by adding the signals.

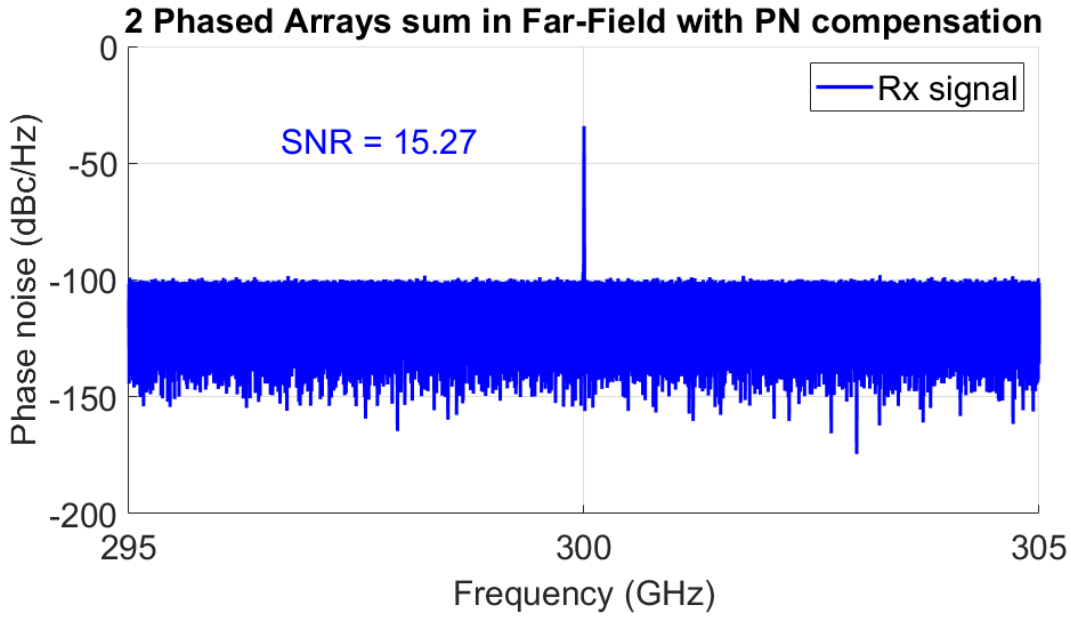

Figure 4.5: Received signal spectrum for two phased arrays with shared LO where array responses are first added at the receiver end and then the resultant signal is compensated for lower offset frequencies.

4.2.2 Simulations with modulated signal

In this section, the simulations for shared LOs have been carried out with SC-QAM modulated signals, and LOs PN spectra can be seen in Figure 4.9 when no PN compensation is involved.

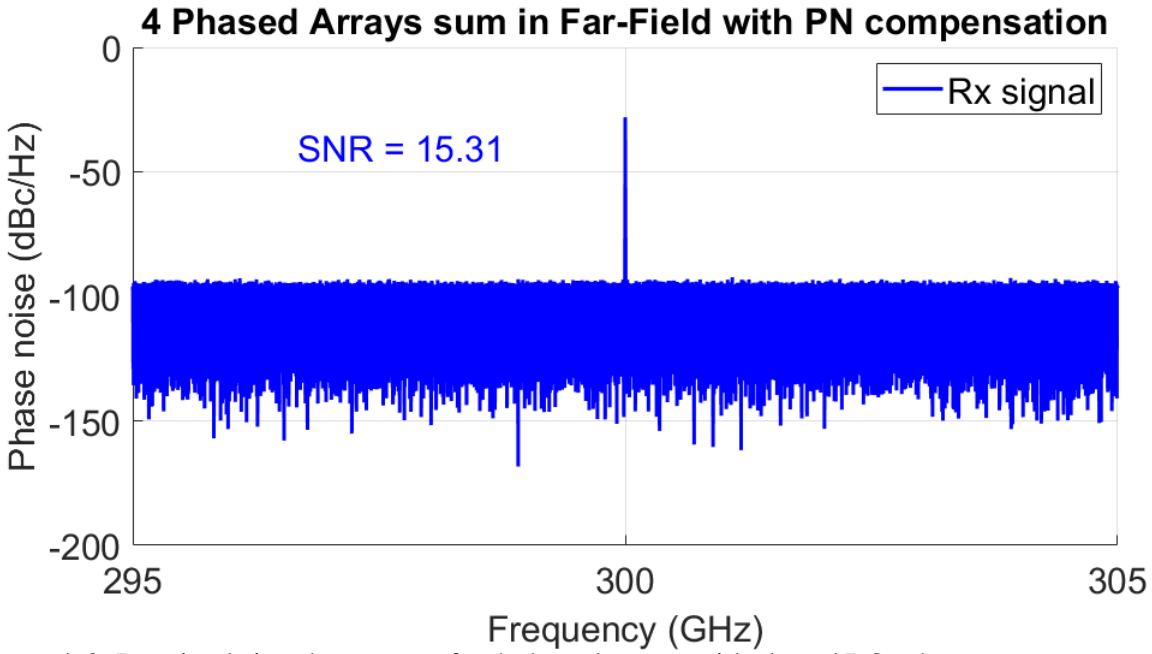

Figure 4.6: Received signal spectrum for 4 phased arrays with shared LO where array responses are first added at the receiver end and then the resultant signal is being compensated for lower offset frequencies.

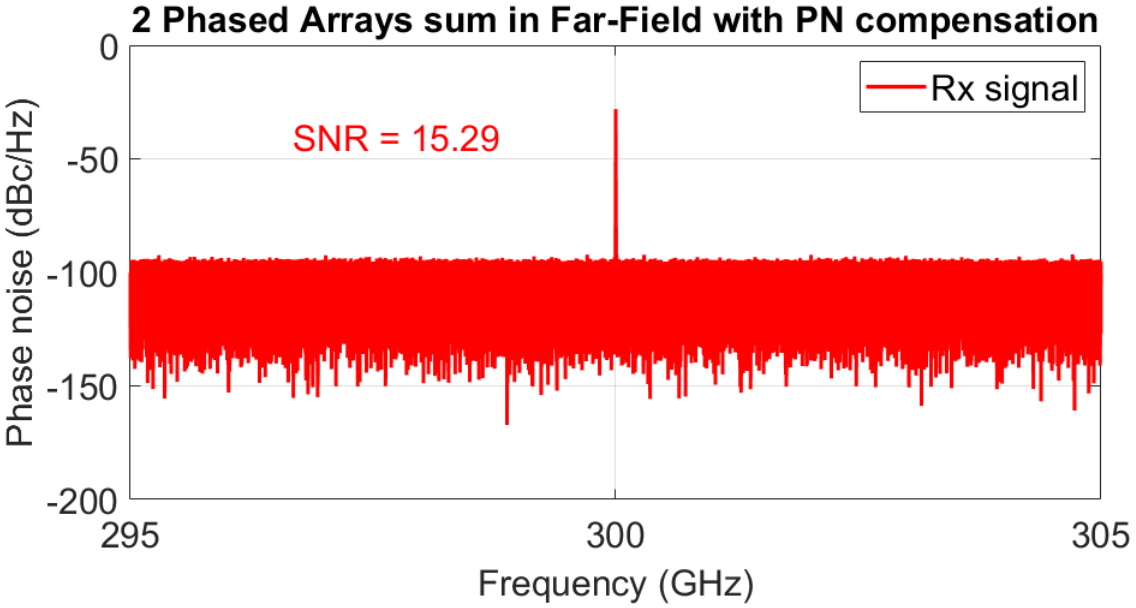

Figure 4.7: Received signal spectrum for two shared LO Case phased arrays where array responses are first compensated independently for lower offset frequencies at the receiver end and then combine the array outputs.

In order to observe the effects of PN on the signal quality of the combined array output, we analyzed the received signal spectrum of the combined array output where the SNR value is dominated by lower offset frequencies which are approximate 15.6 dB and its constellation plot can be seen in Figure 4.10 having EVM approximately 16.55%. We need PN cancellation at a lower offset frequency to see the actual improvement in SNR. In the case where the PN

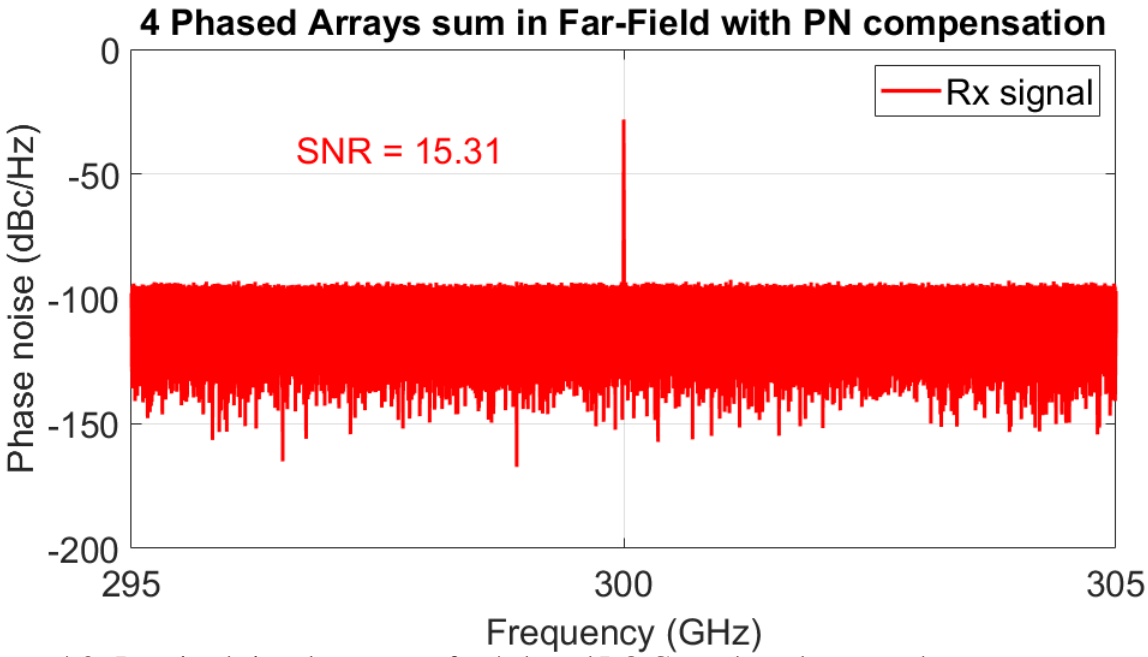

Figure 4.8: Received signal spectrum for 4 shared LO Case phased arrays where array responses are first compensated independently for lower offset frequencies at the receiver end and then combine the array outputs.

compensation is applied to the resultant signal. The two-phased array system performance was improved as can be in Figure 4.11, as the increase in SNR improvement from 15.6 dB to 21 dB and EVM is also decreased from 16.55% to 7.98% which is also can be seen in Figure 4.10 and Figure 4.12, respectively. From these results, we can say that the signal strength has increased significantly, and a much lower level of distortion and noise can be seen with respect to the case when there is no PN compensation involved. Secondly, the scenario where PN compensation is applied to each array response independently and then added to the resultant responses. The SNR value and EVM are almost the same such that., SNR is around 21 dB and EVM is around 8% as shown in Figures 4.15 - 4.16. There is no significant difference in the performance of the system, and it is due to correlated LO noise which is shared to each phased array in this case. The same trend can be seen in the four phased arrays scenario, as shown in Figures 4.13 - 4.14 and Figures 4.17 - 4.18 for both cases when the compensation technique is applied to the resultant signal and in the case where it is applied to each array response independently, which shows the same constant and scalable improvements with the number of phased arrays. A shared LO case illustrates the substantial impact of PN on phased array performance and emphasizes the need to mitigate its effects through appropriate compensation techniques.

4.3 Phase Noise in Multi-Beam Combining with Independent LO Distribution

In the previous section, we discussed different scenarios for shared LO cases with both CW and QAM signals and observe the impact of PN. The simulation will be run in Section 4.3.1 in order to model the effects of PN in multibeam combining for independent LO distribution. The 3GGP PN model has been used in these simulations and the model described in detail in chapter 2 in Section 2.3 as the model can be seen in Figure 2.5 with simulation parameters having a bandwidth of $F_s = 10\,\text{GHz}$ and carrier frequency $F_c = 300\,\text{GHz}$. A detailed examination of

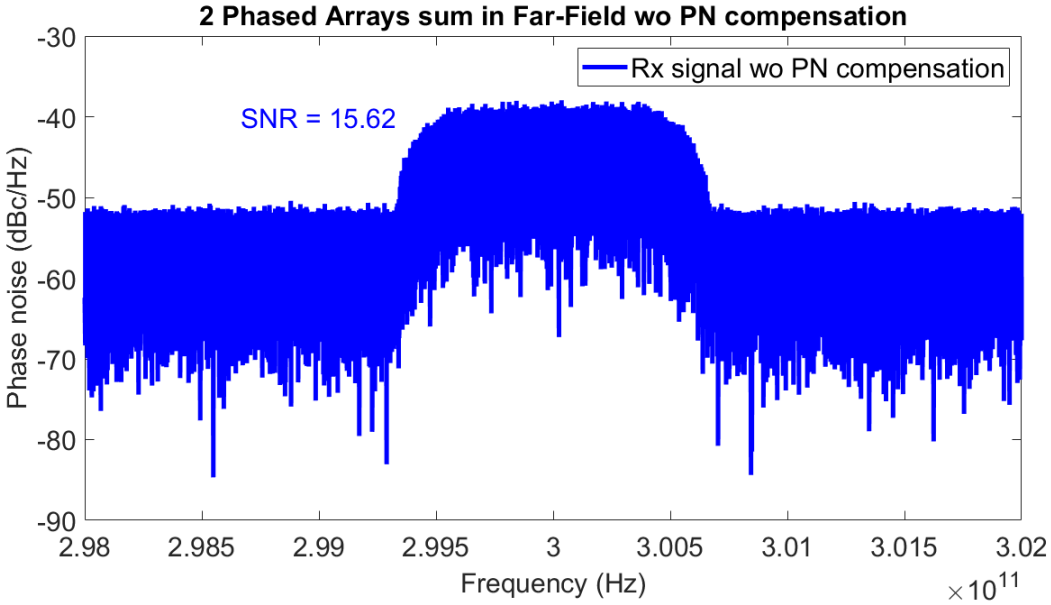

Figure 4.9: Received LO phase noise spectra of two phased arrays sum in the far field for shared LO case with 16 QAM modulated signal and no phase noise compensation involved.

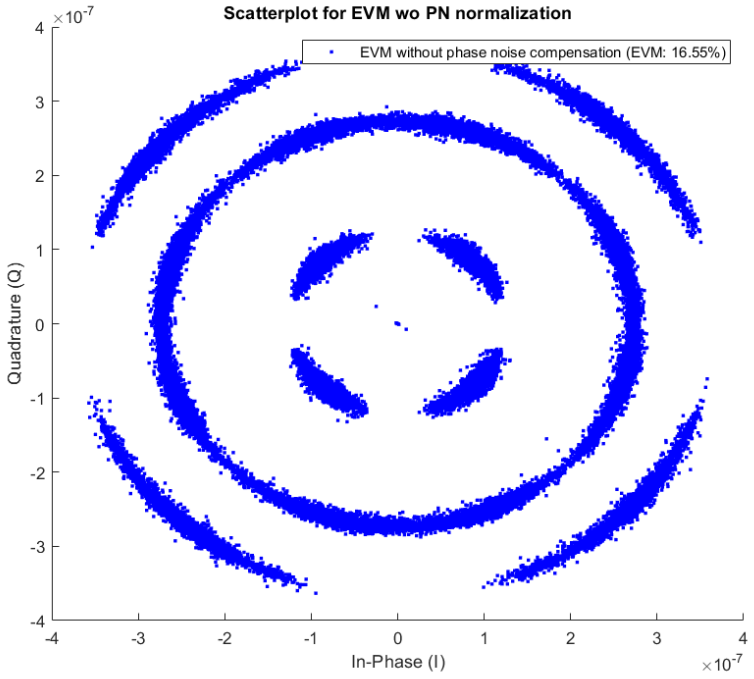

Figure 4.10: Received signal constellation and EVM analysis for LO phase noise for two phased arrays in shared LO case with 16-QAM modulated signal and without phase noise compensation.

the effect on EVM and how the constellation plot can be examined with respect to EVM values for different scenarios, the simulation will be conducted in Section 4.3.2 with a more complex signal such as 16-QAM signal with root raised cosine (RRC) pulse shaping having roll-off factor of (0.35) and symbol rate of 1 GHz. The oversampling factor with the pulse shaping filter is four, which results in four samples per symbol.

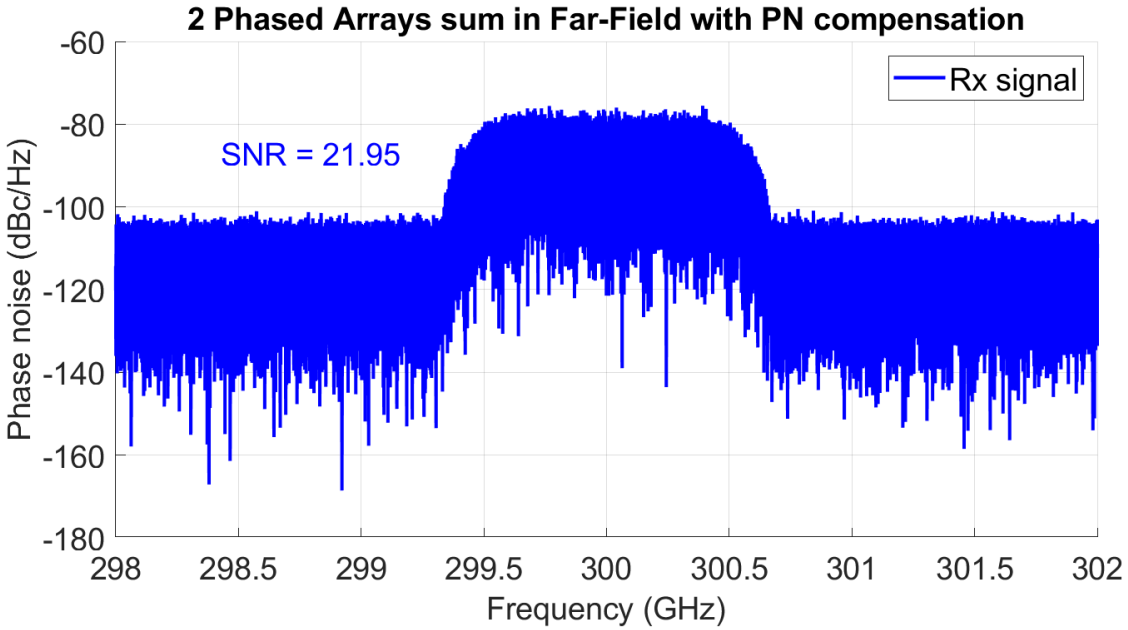

Figure 4.11: Received signal spectrum of two phased arrays summed in the far field for shared LO case with 16-QAM modulated signal and phase noise compensation at low offset frequency (compensating resultant signal after adding array responses at the receiver end).

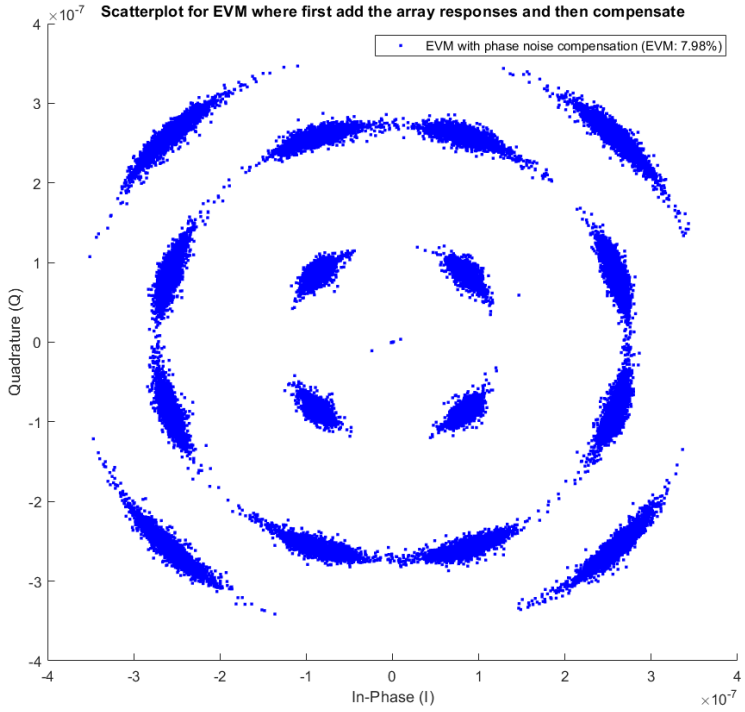

Figure 4.12: Received signal constellation and EVM analysis of two phased arrays summed in far field for shared LO case with 16-QAM modulated signal and phase noise compensation at low offset frequency (compensating resultant signal after adding array responses at the receiver end).

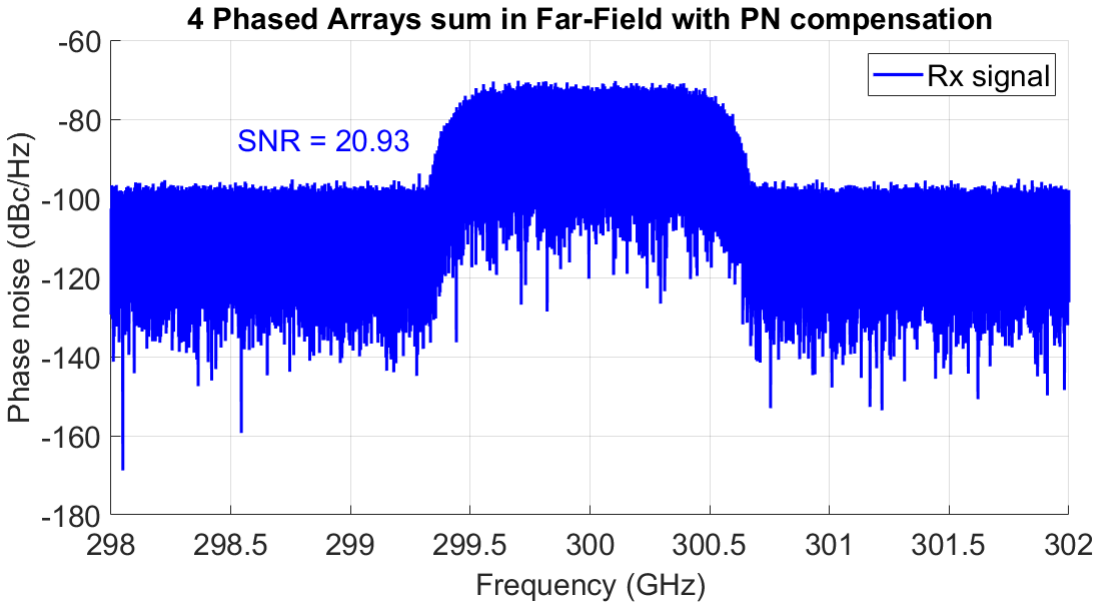

Figure 4.13: Received signal spectrum of 4 phased arrays summed in the far field for shared LO case with 16-QAM modulated signal and phase noise compensation at low offset frequency (compensating resultant signal after adding array responses at the receiver end).

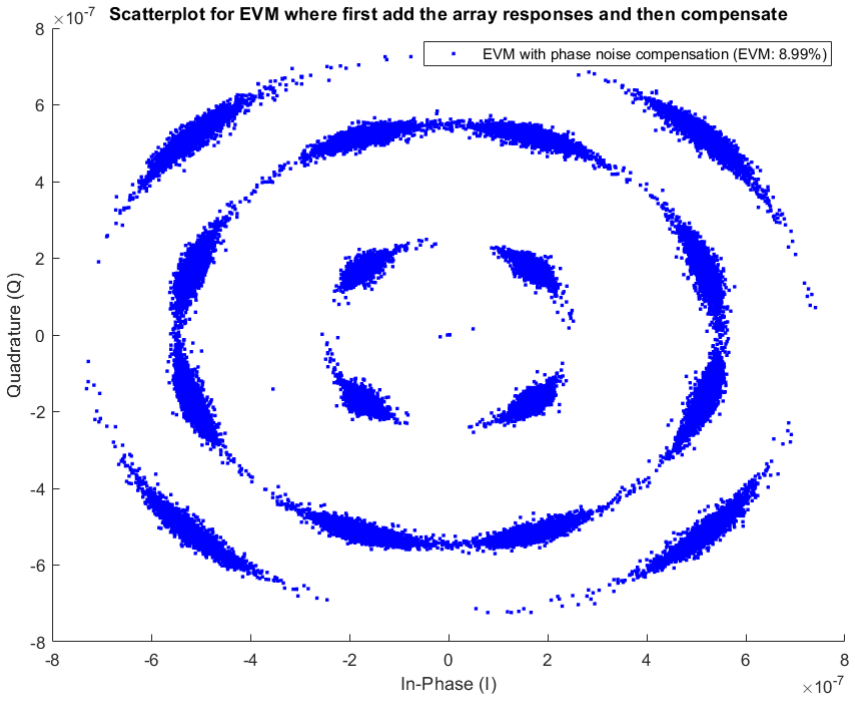

Figure 4.14: Received signal constellation and EVM analysis of 4 phased arrays summed in far field for shared LO case with 16-QAM modulated signal and phase noise compensation at low offset frequency (compensating resultant signal after adding array responses at the receiver end).

4.3.1 Simulations with continuous wave

As can be seen in the below figures, which illustrate three different scenarios, which are analyzed with the aim of how the PN compensation technique impacts the performance of two and four

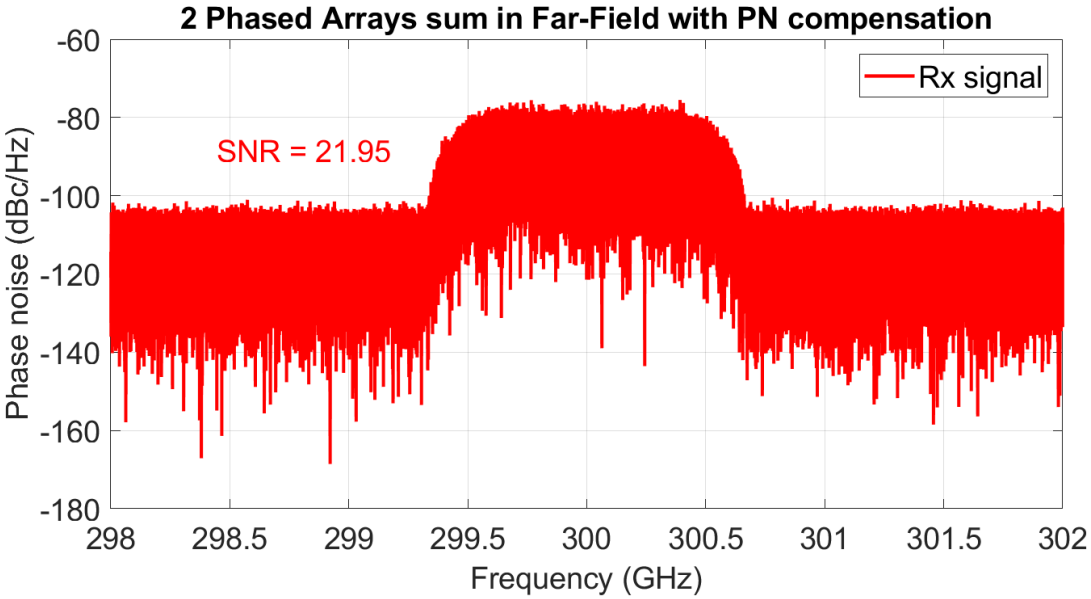

Figure 4.15: Received signal spectrum of two phased arrays summed in the far field for shared LO case with 16-QAM modulated signal and phase noise compensation at low offset frequency (compensating each array response independently before adding array responses at the receiver end).

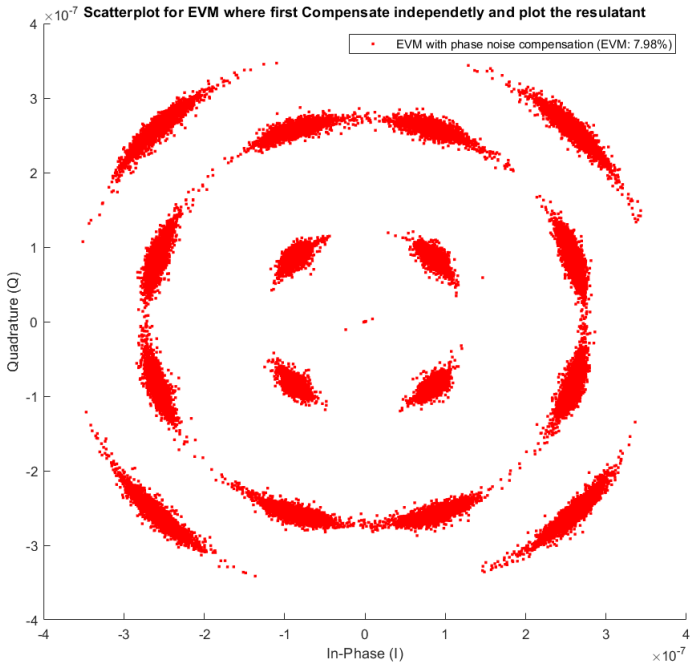

Figure 4.16: Received signal constellation and EVM analysis of two phased arrays summed in the far field for shared LO case with 16-QAM modulated signal and phase noise compensation at low offset frequency (compensating each array response independently before adding array responses at the receiver end).

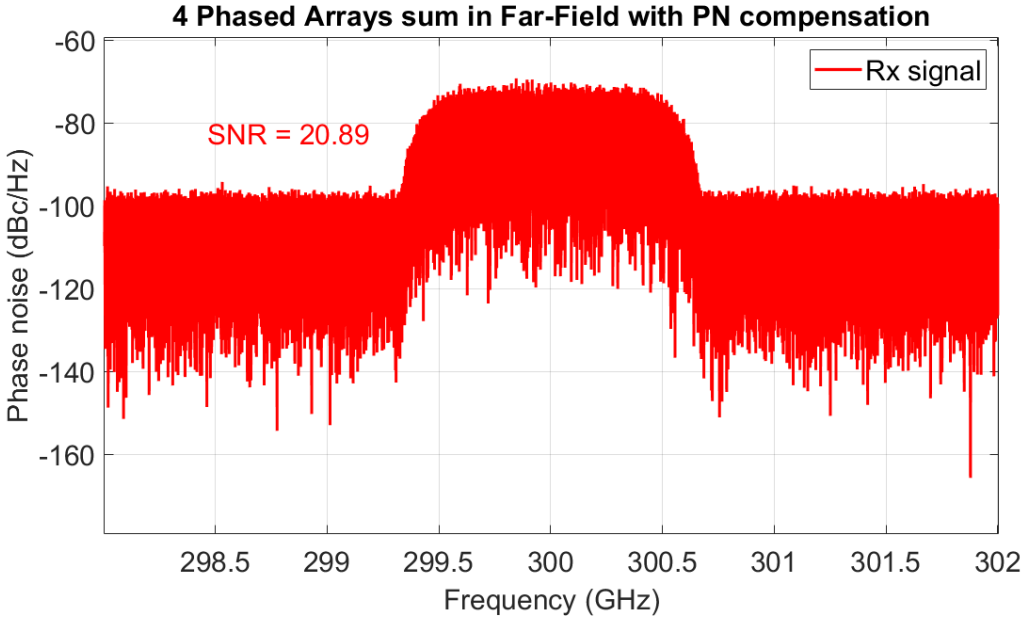

Figure 4.17: Received signal spectrum of 4 phased arrays summed in the far field for shared LO case with 16-QAM modulated signal and phase noise compensation at low offset frequency (compensating each array response independently before adding array responses at the receiver end).

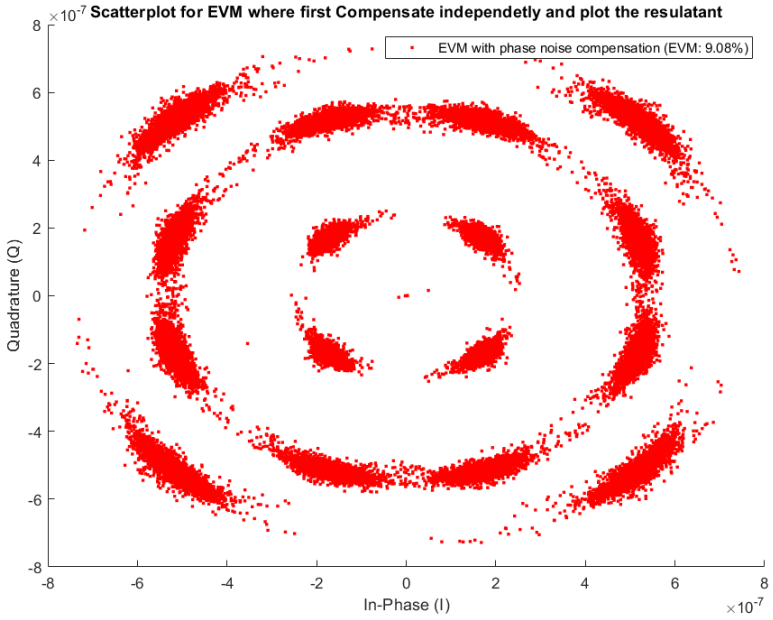

Figure 4.18: Received signal constellation and EVM analysis of 4 phased arrays summed in the far field for shared LO case with 16-QAM modulated signal and phase noise compensation at low offset frequency (compensating each array response independently before adding array responses at the receiver end).

phased arrays with independent LOs means that the noise sources are independent. Figure 4.19 shows LOs PN spectra when there is no PN compensation technique applied and the variation in

SNR value is such that from 2 dB - 20 dB, as shown in Figure 4.22. In the second case where PN compensation is applied to the resultant signal at the receiver end for both two and four phased arrays as illustrated in Figures 4.20 - 4.21. Note that in independent LOs, It was observed that using independent LOs over the antenna elements decreases the signal level due to the fact that the PN sources are independent, and at the receiver end, the independent noise sources can either add up constructively or destructively, thus causing the overall noise power to vary and thus causing the noise power to vary and also the signal power to vary due to noise in the actual signal band i.e., at 300 GHz. A Monte Carlo simulation, both 100 times and 1000 times, was performed to account for this variation. The SNR values achieved for 100 and 1000 simulations ranged from 1.5 dB - 20 dB as shown in Figures 4.22 - 4.23. To account for the problem of array gain, which is due to independent LOs at the receiver end, first, we need to apply the PN compensation technique for each array response separately before adding the resultant signal at the receiver end. Now, as a result, the SNR value for two phased arrays is around 18 dB, and for four phased arrays is approximate 19.50 dB, as shown in Figures 4.24 - 4.25. It makes sure that the signals within the band add constructively when we do PN compensation before combining the result, and signal out of the band which is just incoherent noise so that's why they don't double the noise as the signal doubles.

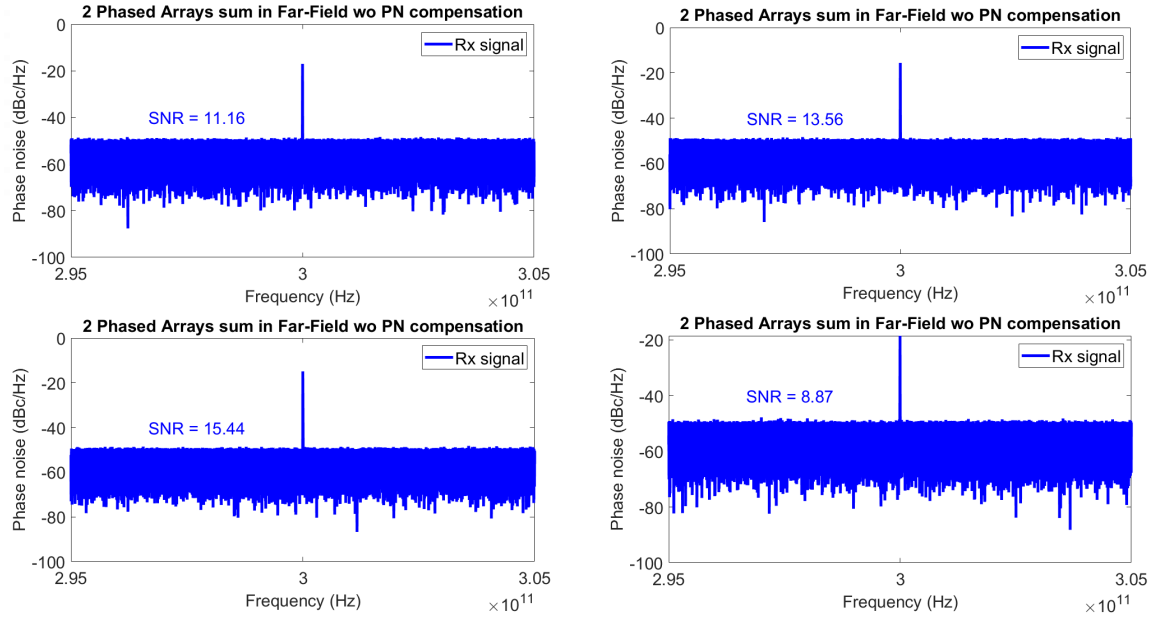

Figure 4.19: Received LO phase noise spectra of 2 phased arrays sum in the far field for independent LO case when there is no phase noise compensation.

4.3.2 Simulations with modulated signal

This section will discuss the same different scenarios discussed in the previous Section 4.3.1 for independent LOs with modulated SC-QAM signals for both two and four phased arrays, as seen in Figure 4.26, where only LO phase noise spectra can be seen as there is no PN compensation involved. The SNR is approximate 19 dB, and the EVM calculation for this SNR value can be seen in the received signal constellation in Figure 4.27, which is around 10.84%. As low SNR

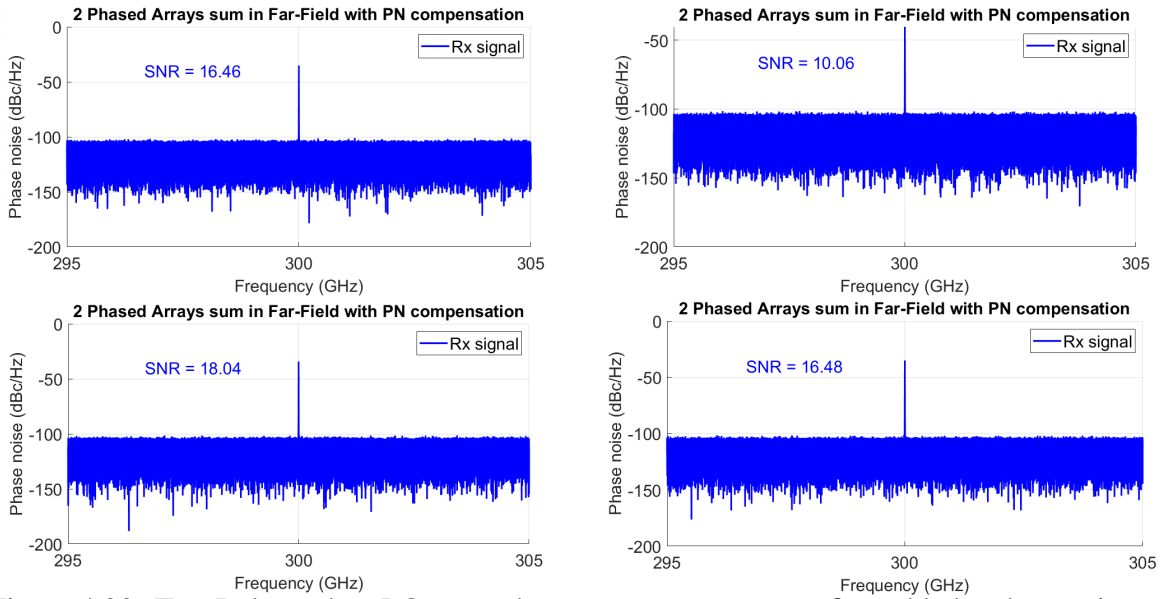

Figure 4.20: Two Independent LO case where array responses are first added at the receiver end and then compensated the resultant for lower offset frequencies.

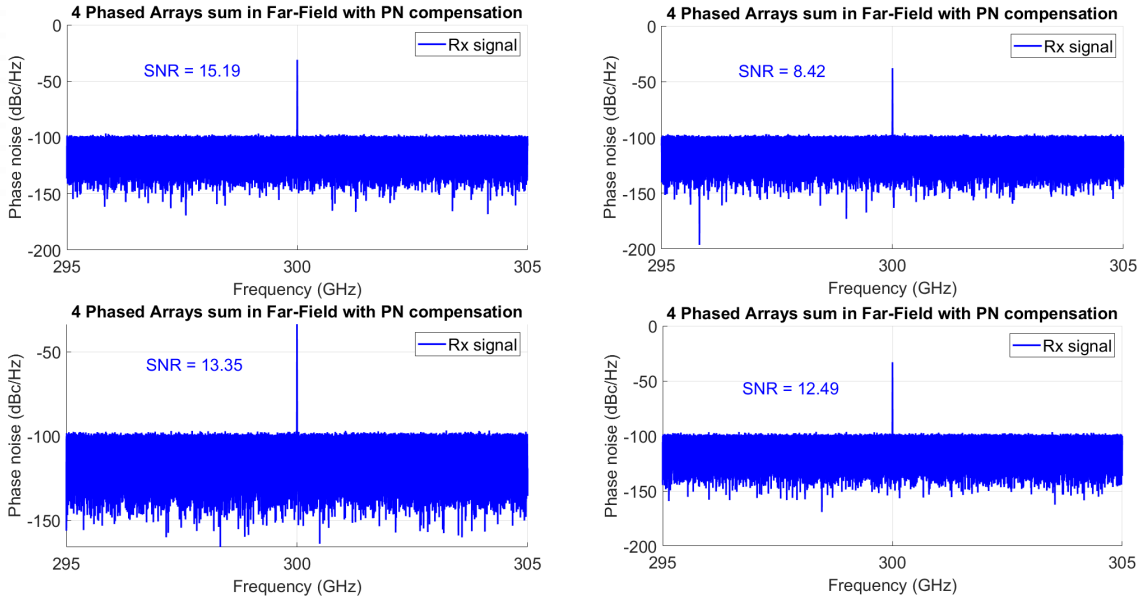

Figure 4.21: 4 Independent LO case where array responses are first added at the receiver end and then compensated the resultant for lower offset frequencies.

and high EVM values indicate that the received signal has a high noise level and low signal quality, we need to apply some phase noise compensation techniques to reduce this effect. We simulated two different scenarios; in the first one, we applied the PN compensation technique after adding the array responses. In the latter case, we first applied PN compensation to each array response independently and then added it to the resultant signal at the receiver end. It can be seen in Figures 4.28 - 4.29 where PN compensation is applied to the resultant signal for two phased arrays with an SNR value of 24.4 dB and an EVM of 6.30% and in Figures 4.30 - 4.31 for four phased arrays having an SNR of 25.5 dB and EVM of 5.26% approximately. The last scenario involves applying PN compensation techniques to each array response independently

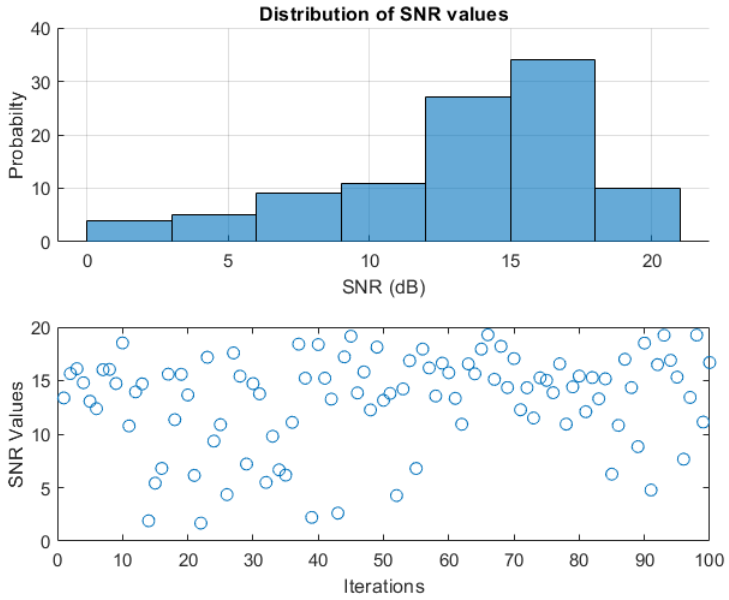

Figure 4.22: Variations in SNR in independent LOs continuous wave signal due to independent noise sources. A Monte Carlo simulation analysis is used to quantify these variations. The Figure illustrate a histogram and realization over 100 times.

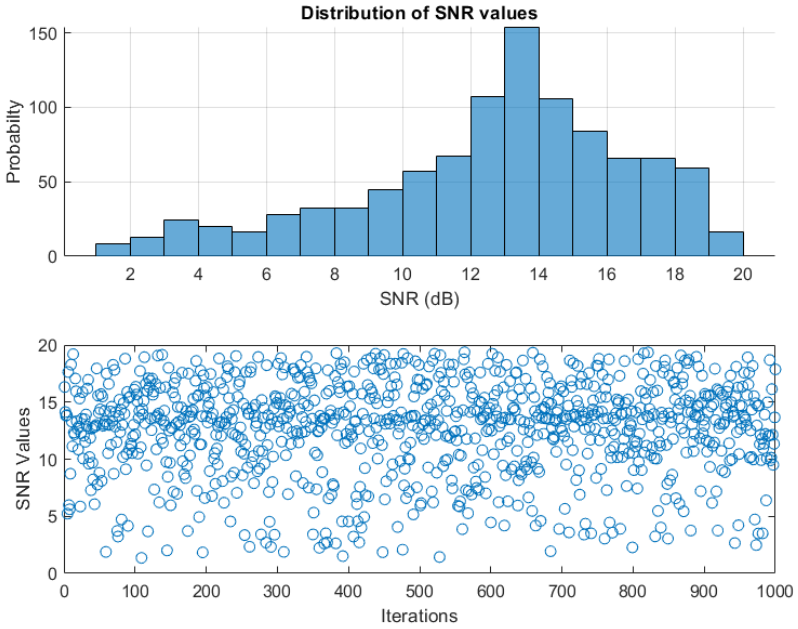

Figure 4.23: Variations in SNR in independent LOs for continuous wave signal due to independent noise sources. A Monte Carlo simulation analysis is used to quantify these variations. The Figure illustrate a histogram and realization over 1000 times.

and adding it to the resultant signal. Figures 4.34 - 4.35 shows two phased array cases with having an SNR of 24.35 dB and an EVM of 6.06%, and in Figures 4.36 - 4.37 for four phased arrays having an SNR of 25.51 dB and an EVM of 5.30% roughly. As in the independent LOs case, we have a problem with array gain since noise sources are independent, which means we

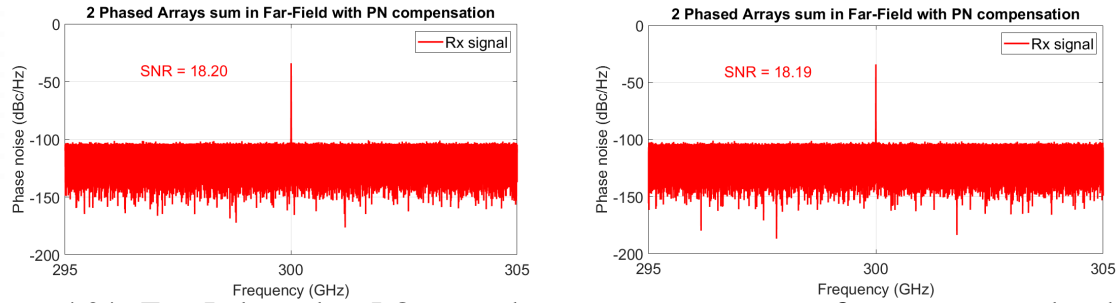

Figure 4.24: Two Independent LO case where array responses are first compensated and then add the resultant at the receiver end for lower offset frequencies.

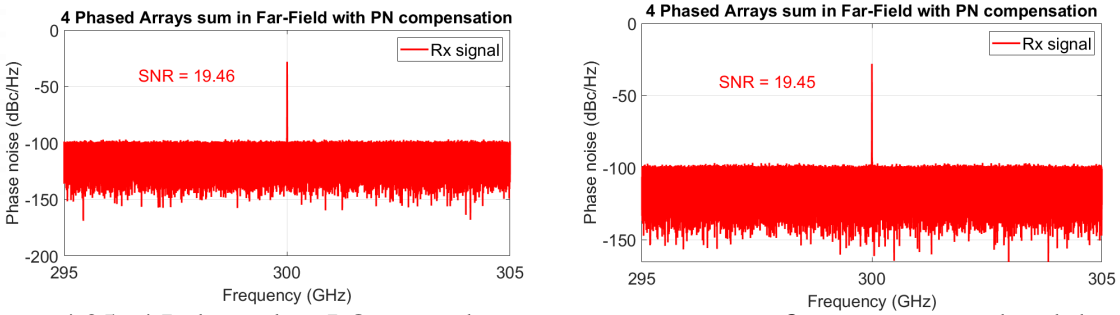

Figure 4.25: 4 Independent LO case where array responses are first compensated and then add the resultant at the receiver end for lower offset frequencies.

might end up with low or even negative SNR. To tackle this issue Monte Carlo simulations for 100 and 1000 realization were performed to catch these SNR fluctuations, as shown in Figures 4.32 - 4.23. It is evident from the comparison of results from the two techniques used in applying for PN compensation independently to each array response before adding the resultant signal. This results in better SNR and EVM results than when we apply the PN compensation techniques after combing it first at the receiver end. So, compensating for PN at the array level helps reduce PN in the signal before it is combined. As we can see PN significantly improves over no compensation from SNR of 19.30 dB to 25.51 dB and EVM from 10.84% to 5.30%. It is concluded from these simulations that time domain PN compensation techniques are precious for improving phased array system performance.

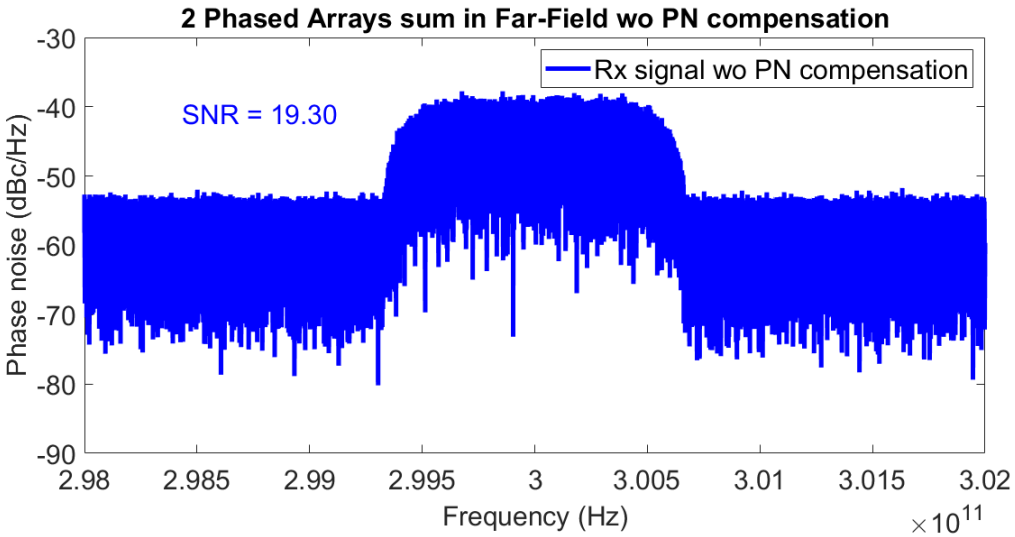

Figure 4.26: Received LO phase noise spectra of two phased arrays sum in the far field for independent LO case with 16 QAM modulated signal and no phase noise compensation involved.

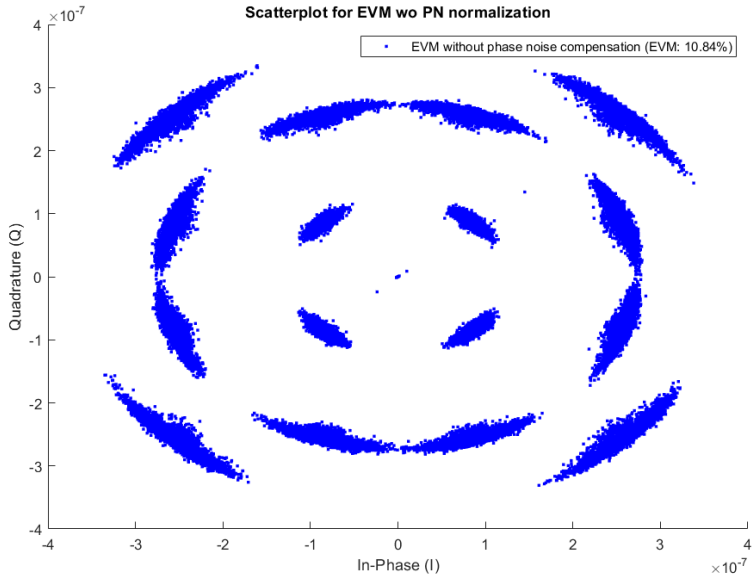

Figure 4.27: Received signal constellation and EVM analysis were conducted for two phased arrays for independent LO phase noise with 16-QAM modulated signal and without phase noise compensation.

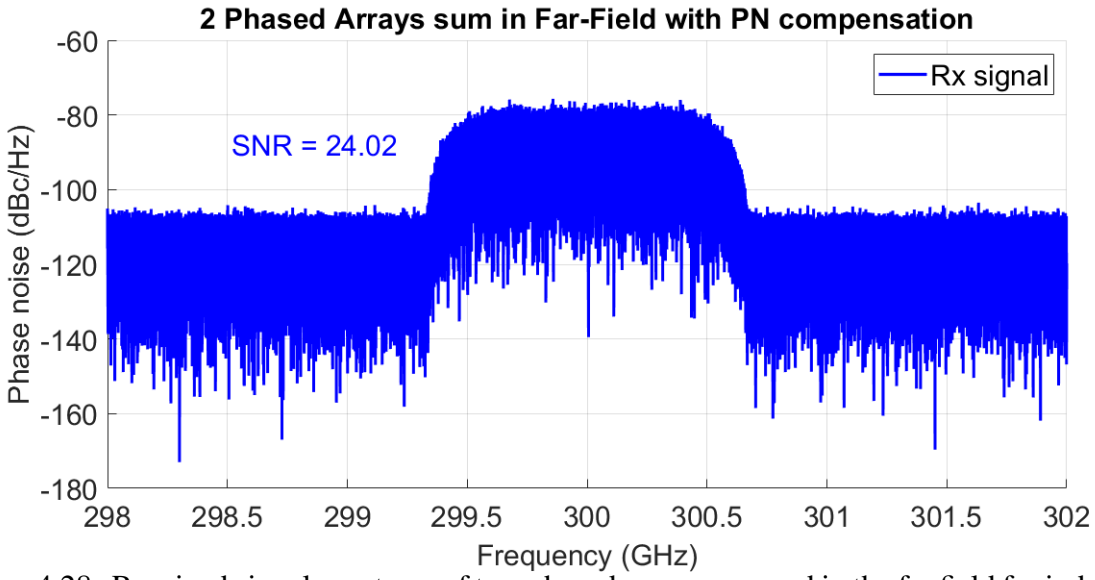

Figure 4.28: Received signal spectrum of two phased arrays summed in the far field for independent LO case with 16-QAM modulated signal and phase noise compensation at the low offset frequencies (compensating resultant signal after adding array responses at the receiver end).

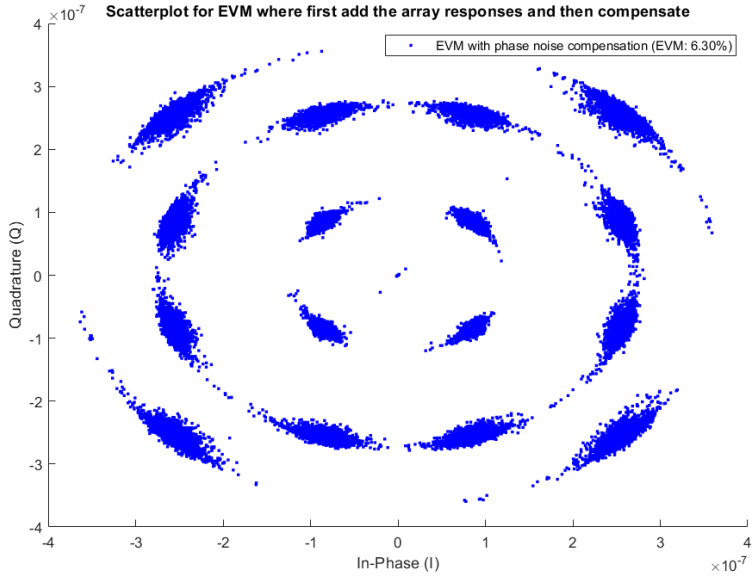

Figure 4.29: Received signal constellation and EVM analysis of two phased arrays summed in the far field for independent LO case with 16-QAM modulated signal and phase noise compensation at the low offset frequencies (compensating resultant signal after adding array responses at the receiver end).

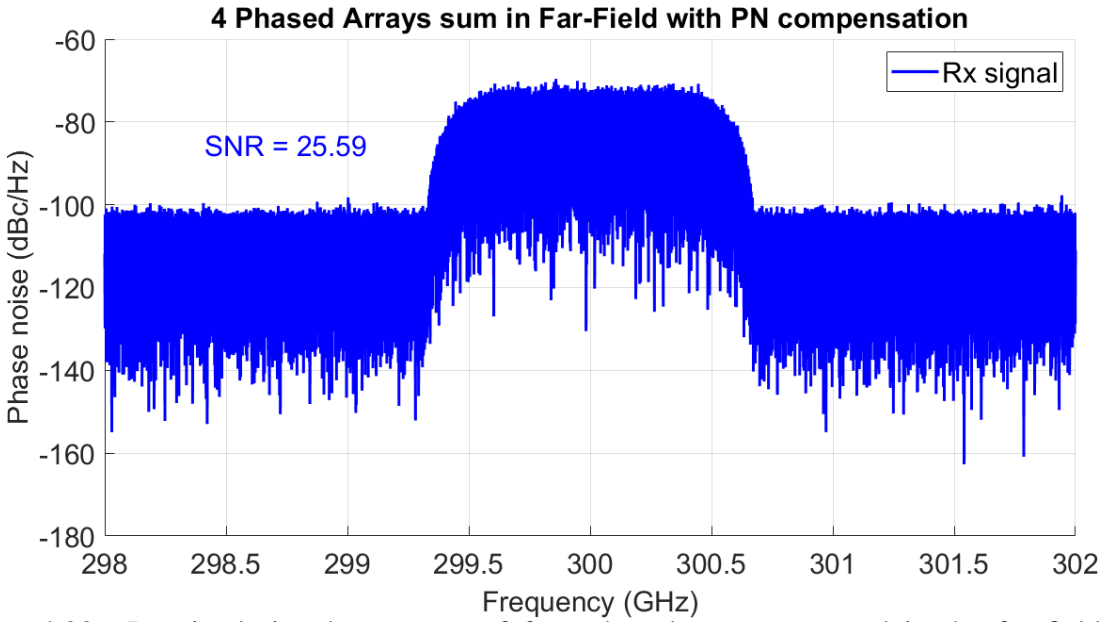

Figure 4.30: Received signal spectrum of four phased arrays summed in the far field for independent LO case with 16-QAM modulated signal and phase noise compensation at the low offset frequencies (compensating resultant signal after adding array responses at the receiver end).

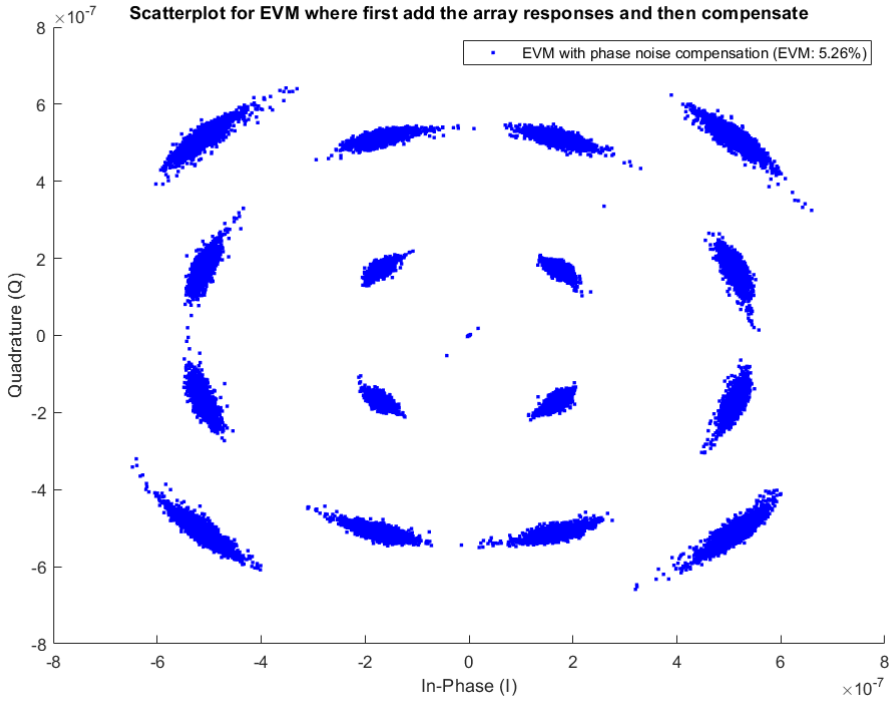

Figure 4.31: Received signal constellation and EVM analysis of four phased arrays summed in the far field for independent LO case with 16-QAM modulated signal and phase noise compensation at the low offset frequencies (compensating resultant signal after adding array responses at the receiver end).

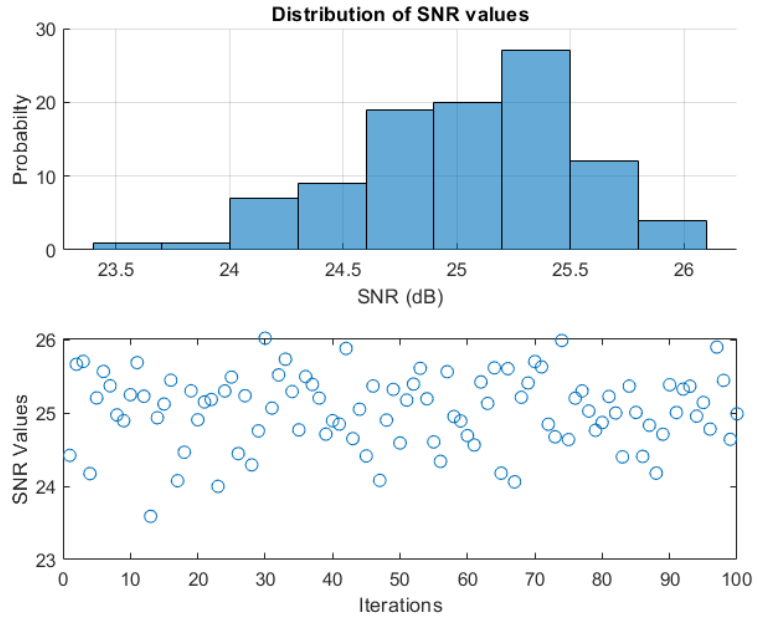

Figure 4.32: Variations in SNR in independent LOs for modulated signal due to independent noise sources. A Monte Carlo simulation analysis is used to quantify these variations over 100 realizations.

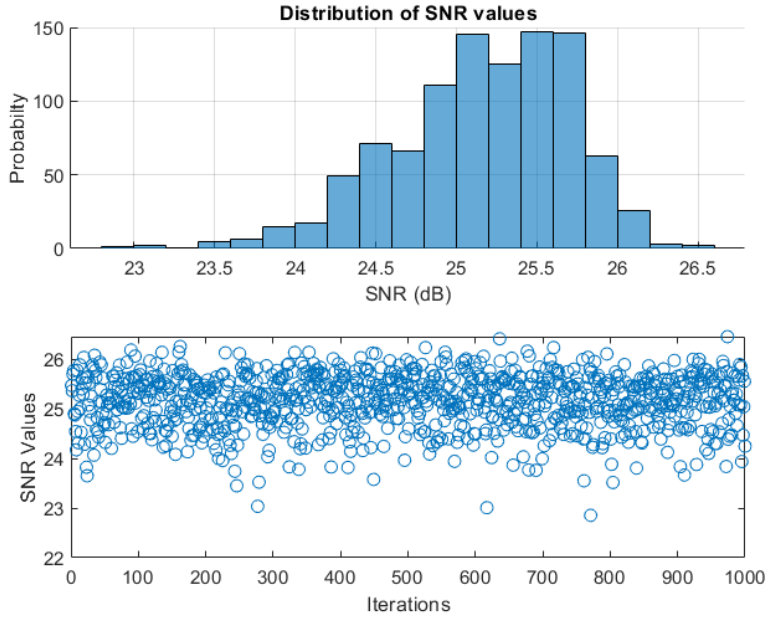

Figure 4.33: Variations in SNR in independent LOs for modulated signal due to independent noise sources. A Monte Carlo simulation analysis is used to quantify these variations over 1000 realizations.

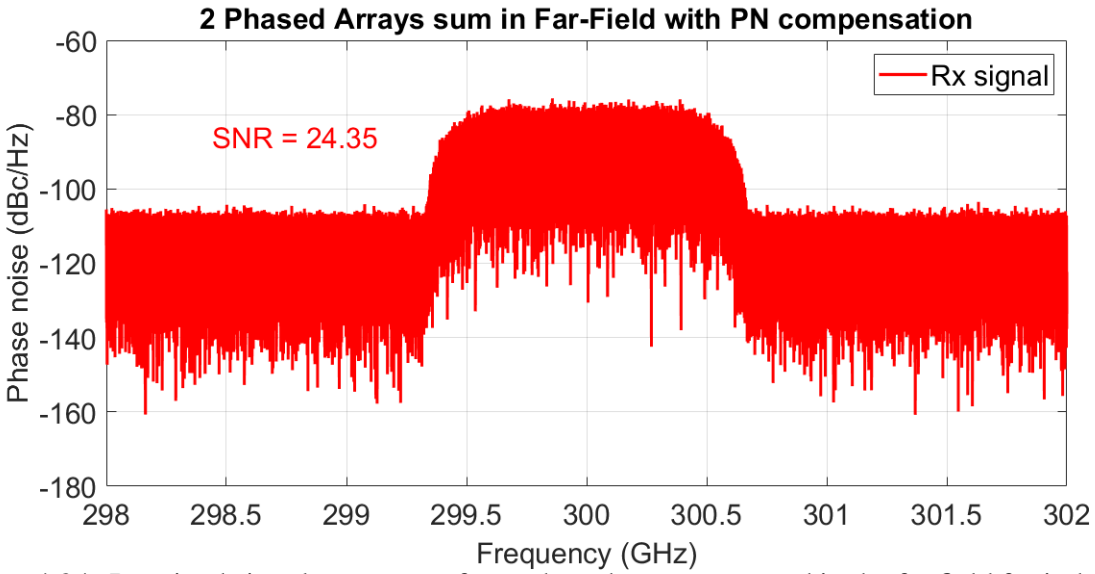

Figure 4.34: Received signal spectrum of two phased arrays summed in the far field for independent LO case with 16-QAM modulated signal and phase noise compensation at the low offset frequencies (compensating each array response independently before adding array responses at the receiver end).

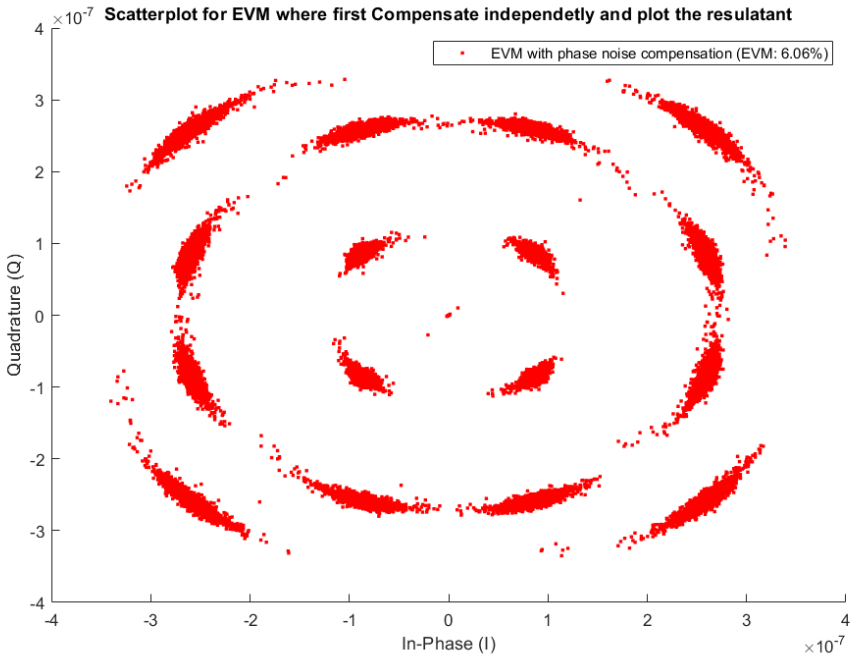

Figure 4.35: Received signal constellation and EVM analysis of two phased arrays summed in the far field for independent LO case with 16-QAM modulated signal and phase noise compensation at the low offset frequencies (compensating each array response independently before adding array responses at the receiver end).

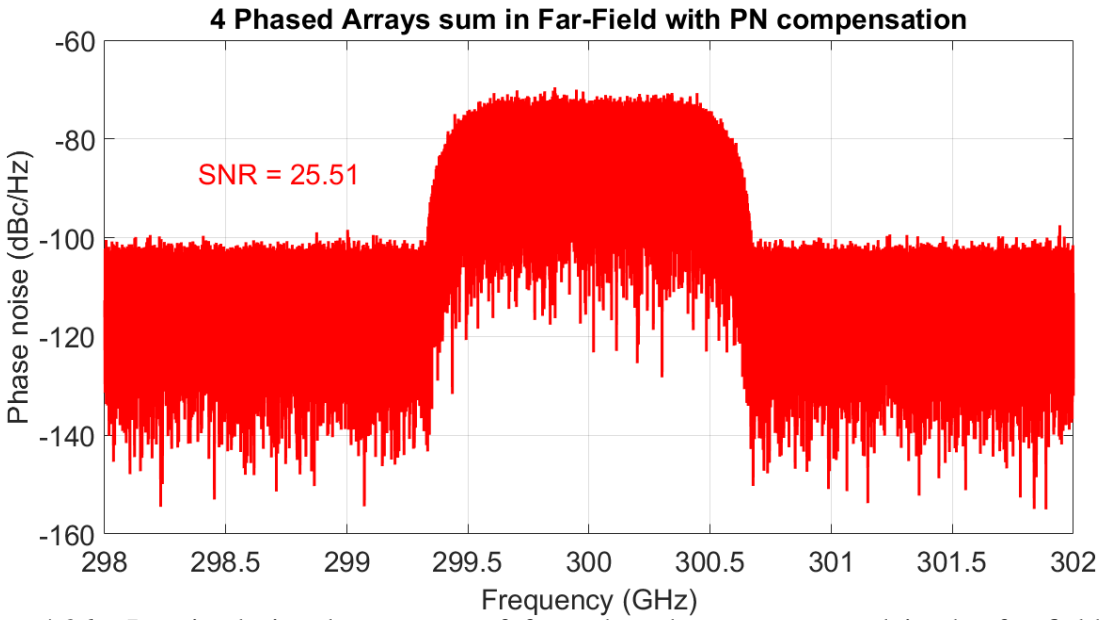

Figure 4.36: Received signal spectrum of four phased arrays summed in the far field for independent LO case with 16-QAM modulated signal and phase noise compensation at the low offset frequencies (compensating each array response independently before adding array responses at the receiver end).

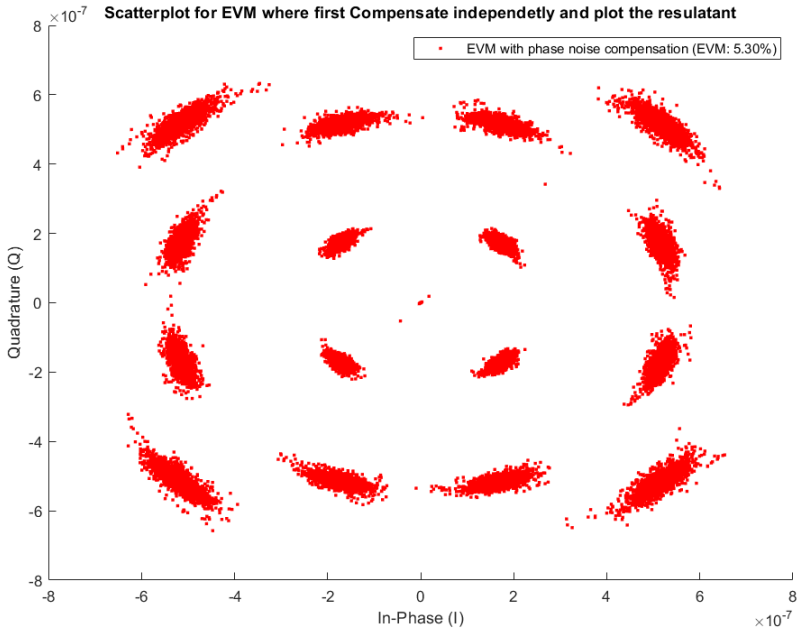

Figure 4.37: Received signal constellation and EVM analysis of four phased arrays summed in the far field for independent LO case with 16-QAM modulated signal and phase noise compensation at the low offset frequencies (compensating each array response independently before adding array responses at the receiver end).

5 CONCLUSION AND DISCUSSION

Understanding and modeling PN are crucial to develop high-performance communication systems. In a communication system, PN occurs when a signal fluctuates in phase, resulting in lowered performance and signal quality. Because of the high carrier frequency and the requirement to achieve accurate beamforming in mmW systems, PN can be particularly challenging. It is imperative to consider stable LO signal generation as an essential factor in mitigating the impact of phase noise in mmW beamforming systems. In order to provide a comprehensive understanding of the issue of phase noise, it is necessary to be able to analyze the behavior of PN in different domains.

A comprehensive analysis of the effect of PN on the mmW beamforming system was presented in this thesis. Chapter 1 discussed the basic motivation and a background overview of PN issues in communication systems. In Chapter 2, several fundamental aspects of PN have been discussed in detail. The impact of PN in mmW phased array system was studied using different LO routing architectures for multi-array transceivers in Chapter 3 and 4. Additionally, two different LO strategies were discussed for multibeam systems, one of which was to use a shared LO distribution network. The other was to use an independent LO distribution network where separate LOs serve each mixer. The simulations use CW signal and SC-QAM waveforms to calculate and compare the EVM improvements. Simulations were performed in MATLAB, as the results are discussed in the next paragraph.

In this thesis phase noise compensation technique is applied in two different ways as discussed previously; first, sum the array responses and apply for sample/symbol level PN compensation to the resultant signal at the receiver end; secondly, first, apply PN compensation to each array response independently and then add the resulting signal. Section 4.2 examines the effect of PN on multibeam combining with shared LO distributions. Simulating with CW signal, compared to the case when there is no PN compensation was applied, the simulations show an 3 dB SNR improvement (from 12.37 dB − 15.27 dB) in SNR when the PN compensation technique was applied to the resultant signal. It was found that both two and four phased arrays did not benefit from the shared LO case when the independent compensation was applied it's because the noise source is correlated. The simulation is also performed with the modulated signal as a result of compensating for PN, SNR, and EVM improvements. When PN compensation was applied to the modulated resultant signal, a significant increase in SNR was achieved from 15.6 dB to 21 dB, and a substantial decrease in EVM was observed from 16.55% to 7.98%. It has been observed that similar results can be obtained by applying for PN compensation independently to each array response before summing the results in the case of the modulated signal.

Section 4.3 examined the impact of PN on multibeam combined with independent LO distributions. Using continuous wave signals for two- and four phased arrays when symbol/sample level PN compensation is applied. It was observed that using independent LOs over the antenna elements decreases the signal level due to the fact that the signals may not combine coherently due to the independent phase noise, which causes variations in SNR values; MC simulations were performed to account for this problem. To overcome the problem of array gain due to independent LOs at the receiver end, PN compensation is applied separately to each array response. This technique results in higher SNR values for both two and four phased arrays, ensuring constructive addition of signals within the band and avoiding noise doubling out of the band, which results in a 18 dB for two-phased and 19 dB for four phased arrays. This SNR improvement is 3 dB more than the shared LO case. For modulated signal, when PN compensation is applied to the resultant signal, there is a significant improvement in SNR and EVM values; two phased arrays have an SNR of around 24.5 dB and an EVM of 6.30%, and for four phased arrays, these values are 25.5 dB and 5.26% calculating PN compensation independently to each array response before summing the results in the case of the modulated signal. For two phased arrays

having an SNR of around 24.35 dB and an EVM of 6.06%, and for four phased arrays, these values are 25.5 dB and 5.26%, which is almost similar to the case when PN compensation is applied to the resultant signal.

To summarize this, it is concluded that in order to increase the signal strength of an array response, PN compensation is applied independently to each array response before adding the resultant signal can benefit more. Using this technique, we achieve better SNR and EVM results than if we combined the PN compensation techniques at the receiver end before applying the PN compensation techniques. So, compensating for PN at the array level helps reduce phase noise in the signal before it is combined. As we can see, PN significantly improves over no compensation from SNR of 15.62 dB to 21.95 dB and EVM from 16.55 % to 7.98 % for shared LO. In addition, SNR improves over no compensation from 19.30 dB to 25.51 dB and EVM from 10.84 % to 5.30 % in independent LO cases. Based on these simulation results, it is concluded that array-level PN compensation techniques are essential for improving phased array systems, but they also increase the complexity of the receiver processing. It is also concluded that the simple level technique works for slow variation, and the array level technique works for fast variation.

Although this study contributed significantly to our understanding of phase noise, future studies should address a few limitations. It is also concluded that the same phase noise in signal paths is the same phase noise in the receiver in one path. Different phase noise in signal paths does not sum entirely coherently, which makes amplitude variations that impact the overall SNR in two different ways: it decreases the overall signal level and adds amplitude noise to it. In the future it may be that it needs to be considered in compensation such that the compensation is not only for a phase but also for amplitude.

6 BIBLIOGRAPHY

[1] Khanzadi M.R. (2015) Phase noise in communication systems–modeling, compensation, and performance analysis. Ph.D. thesis, CHALMERS UNIVERSITY OF TECHNOLOGY.

[2] Pitarokoilis A., Mohammed S.K. & Larsson E.G. (2015) Uplink performance of time-reversal mrc in massive mimo systems subject to phase noise. IEEE Transactions on Wireless Communications 14, pp. 711–723.

[3] Pitarokoilis A. (2013) On the performance of massive MIMO systems with Single Carrier Transmission and Phase Noise. Department of Electrical Engineering, Link ö ping University.

[4] Baghdady E., Lincoln R. & Nelin B. (1965) Short-term frequency stability: Characterization, theory, and measurement. Proceedings of the IEEE 53, pp. 704–722.

[5] Hajimiri A. & Lee T. (1998) A general theory of phase noise in electrical oscillators. IEEE Journal of Solid-State Circuits 33, pp. 179–194.

[6] Aminu M.U., Lehtomäki J. & Juntti M. (2019) Beamforming and transceiver optimization with phase noise for mmwave and thz bands. In: *2019 16th International Symposium on Wireless Communication Systems (ISWCS)*, pp. 692–696.

[7] Pitarokoilis A., Bjornson E. & Larsson E.G. (2015) Optimal detection in training assisted simo systems with phase noise impairments. In: *2015 IEEE International Conference on Communications (ICC)*, pp. 2593–2598.

[8] Durisi G., Tarable A. & Koch T. (2013) On the multiplexing gain of mimo microwave backhaul links affected by phase noise. In: *2013 IEEE International Conference on Communications (ICC)*, pp. 3209–3214.

[9] Zhang W., Gong Y., Zhang X. & Hu Y. (2015) Rf impairments in wireless transceivers: Phase noise, cfo, and iq imbalance – a survey. IEEE Communications Surveys and Tutorials 17, pp. 2229–2267.

[10] Chen X., Fang C., Zou Y., Wolfgang A. & Svensson T. (March 2017) Beamforming mimo-ofdm systems in the presence of phase noises at millimeter-wave frequencies. In: *Proceedings of the 2017 IEEE Wireless Communications and Networking Conference Workshops (WCNCW)*, IEEE, San Francisco, CA, USA, pp. 1–6.

[11] Chen X., Wang H., Fan W., Zou Y., Wolfgang A., Svensson T. & Luo J. (2017) Phase noise effect on mimo-ofdm systems with common and independent oscillators. Wireless Communications and Mobile Computing 2017, pp. 8238234.

[12] Jankovi ć M. & Popovic Z. (2010) Phase noise in microwave oscillators and amplifiers. Ph.D. thesis, University of Colorado, url= `https://www.colorado.edu/faculty/popovic-zoya/sites/default/files/attachedfiles/Thesis_MilosJankovic.pdf`.

[13] Delos P. (2018), System-level lo phase noise model for phased arrays with distributed phase-locked loops. url=https://www.analog.com/en/technical-articles/system-level-lo-phase-noise-model-for-phased-arrays-with-distributed-phase-locked-loops.html.

[14] Erik Dahlman Stefan Parkvall J.S. (2020) 1.chapter 26, §26.2: “mmw lo generation and phase noise aspects”. 5G NR - The Next Generation Wireless Access Technology, 2nd Edition pp. 527–533.

[15] Chen J., He Z.S., Kuylenstierna D., Eriksson T., Hörberg M., Emanuelsson T., Swahn T. & Zirath H. (2017) Does lo noise floor limit performance in multi-gigabit millimeter-wave communication? IEEE Microwave and Wireless Components Letters 27, pp. 769–771.

[16] Puglielli A., LaCaille G., Niknejad A.M., Wright G., Nikolic B. & Alon E. (2016) Phase noise scaling and tracking in ofdm multi-user beamforming arrays. In: *2016 IEEE International Conference on Communications (ICC)*, pp. 1–7.

[17] Telba A., Noras J., Eta M.E. & Mashary B.A. (2004) Simulation technique for noise and timing jitter in phase locked loop. In: *Proceedings of the 16th International Conference on Microelectronics, 2004*, IEEE, pp. 505–508.

[18] Mavridis D. & Efstathiou K. (2006) A vco’s phase-noise reduction technique. In: *2006 Ph.D. Research in Microelectronics and Electronics*, pp. 101–104.

[19] Bicaïs S. & Doré J.B. (December 2019) Phase Noise Model Selection for Sub-THz Communications. In: *IEEE Global Communications Conference 2019*, Waikoloa, United States.

[20] Kamal A., Mahmoud A. & Sharaf K. (May 2004) Low phase noise vco design - a thesis. Ph.D. thesis, Ain shams University.

[21] Lee T. & Hajimiri A. (2000) Oscillator phase noise: a tutorial. IEEE Journal of Solid-State Circuits 35, pp. 326–336.

[22] Kester W. (01 2005), Converting oscillator phase noise to time jitter.

[23] Weist F. (2023) Phase-noise modeling, simulation, and propagation in phase-locked loops: Part 1. Electronic Design .

[24] 3GPP TR 38.800: Study on Phase Noise in 5G NR. `https://www.3gpp.org/ftp//Specs/archive/38_series/38.800/38800-920.zip`, Accessed: December 22, 2022.

[25] Hexa-X (2022) Initial radio models and analysis towards ultra-high data rate links in 6g. Deliverable D2.2, url = `https://hexa-x.eu/wp-content/uploads/2022/01/Hexa-X-D2_2.pdf`.

[26] Litinskaya Y.A., Alexandrin A.M., Lemberg K.V., Polenga S.V. & Salomatov Y.P. (2013) Phased array antenna with combined electronical and mechanical beam steering for satellite networks. In: *2013 International Siberian Conference on Control and Communications (SIBCON)*, IEEE, pp. 1–3.

[27] Khan M., Anab M., Khan M.K., Ur Rahman S. & Sultan A. (06 2021) A survey on beam steering techniques in printed antennas. International Journal of Recent Contributions from Engineering, Science & IT (iJES) 9, pp. 4.

[28] Jeon S., Wang Y.J., Wang H., Bohn F., Natarajan A., Babakhani A. & Hajimiri A. (2008) A scalable 6-to-18 ghz concurrent dual-band quad-beam phased-array receiver in cmos. IEEE Journal of Solid-State Circuits 43, pp. 2660–2673.

[29] Haupt R.L. (2019) Lowering the sidelobe level of a two-way array factor for an array with uniform transmit and uniform receive arrays. IEEE Transactions on Antennas and Propagation 67, pp. 4253–4256.

[30] Hamza N. (2022) Modeling analog signal routing for wideband mmw phased arrays. Master's thesis, University of Oulu, url = http://jultika.oulu.fi/files/nbnfioulu-202207013230.pdf.

[31] Yasir M. (2017) Characterizing nonlinearity in multiantenna multibeam transmitters. Master's thesis, University of Oulu, url = http://jultika.oulu.fi/files/nbnfioulu-201712053277.pdf.

[32] Balanis C.A. (2016) Antenna theory: analysis and design. In: *Antenna Theory: Analysis and Design*, John Wiley & Sons, pp. 619–623.

[33] Mathecken P., Riihonen T., Werner S. & Wichman R. (01 2011) Performance analysis of ofdm with wiener phase noise and frequency selective fading channel. IEEE Transactions on Communications 59, pp. 1321–1331.

[34] KIM M., ichi TAKADA J. & SAITO K. (2018) Multi-dimensional radio channel measurement, analysis and modeling for high frequency bands. IEICE Transactions on Communications E101.B, pp. 293–308.

[35] Chen X., Wang H., Fan W., Zou Y., Wolfgang A., Svensson T. & Luo J. (11 2017) Phase noise effect on mimo-ofdm systems with common and independent oscillators. Wireless Communications and Mobile Computing 2017.

[36] LaCaille G., Puglielli A., Alon E., Nikolic B. & Niknejad A. (11 2019) Optimizing the lo distribution architecture of mm-wave massive mimo receivers. arXiv: Signal Processing .

[37] Rasekh M.E., Abdelghany M., Madhowz U. & Rodwell M. (2019) Phase noise analysis for mmwave massive mimo: a design framework for scaling via tiled architectures. In: *2019 53rd Annual Conference on Information Sciences and Systems (CISS)*, pp. 1–6.

[38] Easwaran U. & Krishnaveni V. (Jul 2022), Analysis of phase noise issues in millimeter wave systems for 5g communications - wireless personal communications.

[39] Rasekh M.E., Abdelghany M., Madhow U. & Rodwell M. (2021) Phase noise in modular millimeter wave massive mimo. IEEE Transactions on Wireless Communications 20, pp. 6522–6535.

[40] Fang Y., Qiu L., Liang X. & Ren C. (2021) Cell-free massive mimo systems with oscillator phase noise: Performance analysis and power control. IEEE Transactions on Vehicular Technology 70, pp. 7296–7308.

[41] Barb G., Otesteanu M., Alexa F. & Ghiulai A. (2020) Digital beamforming techniques for future communications systems. In: *2020 12th International Symposium on Communication Systems, Networks and Digital Signal Processing (CSNDSP)*, pp. 1–4.

[42] Kasemir P., Sutton N., Radway M., Jeong B., Brown T. & Filipovič D.S. (2009) Wideband analog and digital beamforming. In: *2009 9th International Conference on Telecommunication in Modern Satellite, Cable, and Broadcasting Services*, pp. 372–375.

[43] Spalvieri A. & Barletta L. (2011) Pilot-aided carrier recovery in the presence of phase noise. IEEE Transactions on Communications 59, pp. 1966–1974.

[44] 3GPP Series 38. https://www.3gpp.org/dynareport?code=38-series.htm, Accessed: January 14, 2023.

[45] Afshang M., Hui D., Cheng J.F.T. & Grant S. (2022) On phase noise compensation for ofdm operation in 5g and beyond. In: *2022 IEEE Wireless Communications and Networking Conference (WCNC)*, pp. 2166–2171.

[46] Wikipedia (2004), Moving average. https://en.wikipedia.org/wiki/Moving_average, Accessed: January 08, 2023.